MIMO Testing Methodologies

by

Marcos A. Underwood, Ph.D.
Spectral Dynamics (SD), Inc.

and

Michael Hale, Ph.D.
Dynamic Test Branch, Redstone Technical Test Center (RTTC)

This paper will discuss some recent MIMO testing that was performed to compare the results that are possible with: under-defined square control, optimal square control, rectangular control, and I/O transformation control. Two types of test profiles were used for this study: Haystack References for X, Y, and Z; and MIL-STD-810G profiles for X, Y, and Z. In all of these tests, the objective is to drive the X, Y, and Z axes such that the respective axis response agrees with their pre-specified reference PSD, and such that the respective axis responses are incoherent with each other.

These tests were performed at the Dynamic Test Branch of RTTC, with the use of a Team Cube Model 3 DOF actuator system and the SD Jaguar MIMO control system. The objective of the study is to compare these four types of testing methodologies, by discussing their relative strengths and weakness of the various testing approaches, thus providing a methodology to the general community for selecting amongst test methods.

The study shows that for cases in which spectral content associated with flexible body dynamics related to either the excitation system and/or payload falls within the test bandwidth; that both Rectangular and I/O Transformation MIMO control methodologies result in more uniform and more accurate MIMO Random environmental simulations. The combination of equipment used to conduct the tests also demonstrated a great degree of robustness and stability during the controlled testing process, which also yielded very repeatable results. This indicates that these methodologies are ready for general usage.

The test results also show that MIMO testing can be used to accomplish tests such as the MIL-STD-810G profiles more efficiently and more realistically. The increase in efficiency is a result of testing three axes simultaneously rather than testing them sequentially as is usually done. It's also more realistic since the environments that most test articles experience is multi-axes, which is not adequately simulated when testing one axis at a time.

Introduction

The tests used for the study were conducted using MIMO random[1] because of the increased visibility that this testing methodology provides in assessing performance. We were interested in determining what the performance envelope of the Team Cube was in this application and the levels at which it could run a 3-D version of the newest Mil-STD-810G[2] profiles that are discussed in its section: METHOD 514.6 ANNEX C, for the traditional one-axis-at-a-time testing. We knew that we would be pushing the Cube's testing capabilities and thus are also interested to find if we could optimize various parameters of the tests to further enhance the Cube's testing capabilities.

We also wanted to see what type of 6-DOF testing performance could be obtained with the Cube and the use of MIMO control. For this, we decided to compare the test results obtained with the use of square control,[1] both underdefined[3] and optimal;[3] rectangular control;[4] and I/O transformation control.[5]

Control Methods

Square 6-DOF MIMO random control is achieved by controlling the Cube's 6 actuators with the use of 6 accelerometers, where the control system is tasked with finding a vector of drive signals, which are used to drive the actuators, such that the control-response SDM[6] of the control accelerometers match a predetermined reference SDM, within an acceptable error tolerance.[1] In the under defined case, the 6 control accelerometers are located on a line and in the optimal case, the accelerometers are located in such a way as to form a plane, on the top surface of the Cube.

Rectangular control is when we use more than 6 accelerometers to control the Cube's 6 actuators. In this case, the MIMO control system needs to find a vector of drive signals, with which to drive the Cube's 6 actuators, such that the control-response SDM of the control accelerometers match a predetermined reference SDM, within an acceptable error tolerance *in the least-squares sense, for all of the respective elements of the control and reference SDMs*.[4] We used 12 control accelerometers for these tests.

For the Cube, I/O transformation control uses an input transformation[5] to convert the control accelerometer response signals into equivalent 6-DOF responses in the X, Y, and Z axis as, well as the rotations about the X, Y, and Z axis, which we call R_x (roll), R_y (pitch), and R_z (yaw). The MIMO control system controls the 6-DOFs by again finding a vector of drive signals that cause the SDM of the *transformed* responses of the control accelerometers to match a predetermined reference SDM, which describes the desired 6-DOF motion at the top surface of the Cube, in terms of the aforementioned DOFs.[5] This control method in general also requires an output transformation,[5] but since the Cube is capable of actuating 6-DOFs, a unity output transformation is used. This can be done because the impedance matrix,[1] [Z(f)], can also be used to perform the necessary rigid-body geometric transformation from the 6-DOF motion space to the Cube's actuator space, as well as the needed dynamic cross-coupling compensation, as a function of frequency, which is its usual function.[1] We also used 12 control accelerometers for these tests.

Instrumentation

The top surface of the cube was instrumented using four tri-axial accelerometers, with one tri-ax at each of the Cube's corners. The four corners are numbered 1 through 4 as shown in the following Fig. 1, which shows their orientation with respect to our chosen right-hand coordinate system (X,Y,Z).

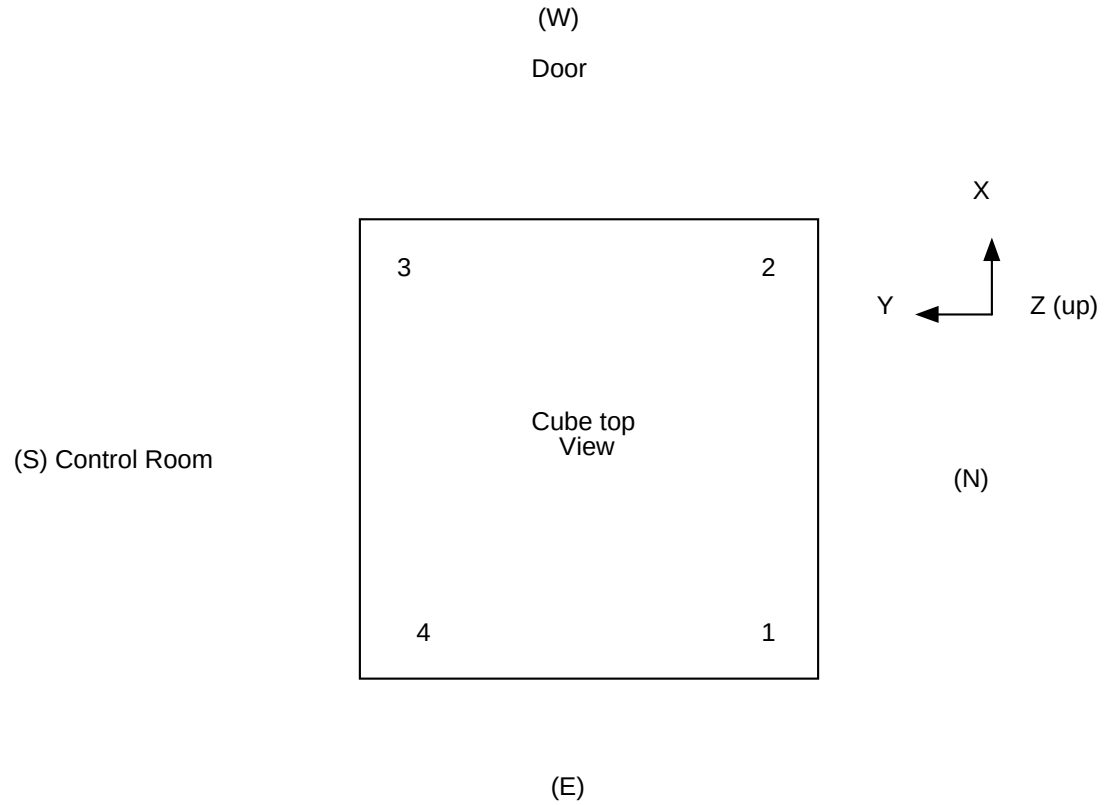

Fig. 1: Plan view of the top surface of the Team Cube as installed in test lab.

Testing

In the following discussion, we will refer to the various control accelerometers that were used for the various tests that were performed, by the axis in which it points and with the corner number as its subscript. For example the x-axis accelerometer at corner three in Fig. 1 is called accelerometer x_3.

In the following, most tests use a maximum performance haystack spectrum, which is defined to achieve the maximum stroke, velocity, and acceleration limits of the Cube, unless otherwise specified. The following types of tests were performed:

1) Square control using two tri-axial accelerometers mounted at corners 1 and 3, and with zero coherence[6,7,8] between their respective responses. This type of instrumentation choice results in the accelerometer locations being co-linear and thus unable to uniquely determine the 6-DOF motion of a plane. For this reason, this type of test will be called under-defined square control in the following discussion. However, since the motion of the 6 accelerometers can be independent, MIMO control can cause the responses to be incoherent.[1,6] Thus, a form of 6-DOF motion should occur as a result, but with roll and pitch being linearly dependent.[3]

2) Under-defined square control, at control locations 1 and 3, but with 0.95 coherence between pairs of X, Y, and Z responses. In this case, nearly pure 3-DOF motion should occur,[6] but with some uncontrolled roll and pitch, due to the under-defined nature of the chosen instrumentation configuration.

3) Under-defined square control, at locations 1 and 3, 0.95 coherence between pairs of X, Y, and Z responses, but with the Y and Z responses at $1/10^{th}$ the amplitude of the X response. In this case, nearly pure X motion should occur, but with less uncontrolled roll and pitch than in test 2), due to the Z responses being low with respect to X responses.

4) Optimal square control that used x_1, y_1, z_1, y_2, z_2, and z_3 for control, with 0.95 coherence between the two Y accelerometer's and between the three Z accelerometer's responses (pure X, Y, Z uncorrelated);

5) Optimal Square control, using the same control accelerometers as in 4), and the same coherence relationship, but with 180^o phase between the y_1 and y_2 responses and with 180^o phase between the z_1 and the z_2 and z_3 responses (pure Roll and Yaw uncorrelated);

6) Optimal Square control using the MIL-STD-810G[2] reference shape for the X, Y, and Z profiles, with 0.95 coherence between the respective Y responses and between the respective Z responses (pure X, Y, and Z uncorrelated);

7) Rectangular control using the all 4 tri-axial accelerometers for control with the respective MIL-STD-810G reference for each of the X, Y, and Z controls, and with 0.95 coherence between each of the X, Y, and Z accelerometers (pure X, Y, and Z uncorrelated);

8) I/O transformational control using the same instrumentation as 7), but 0 coherence between the control DOFs, and with an input transformation[5,9,10] to reduce the control DOFs into X, Y, Z, Roll, Pitch, and Yaw responses.

9) I/O transformational control using the same instrumentation as 8), but with the use of MIL-STD-810G reference shapes for the X, Y, and Z axes. As in 8), 0 coherence between the control DOFs is specified and with an input transformation to reduce the control DOFs into X, Y, Z, Roll, Pitch, and Yaw responses.

The following table summarizes the above tests and their associated control channels:

Test Type	Control Accels
1) Under-defined square with 0.0 coherence between controls and with max performance haystack spectrum for all controls	x_1, x_3, y_1, y_3, z_1, z_3
2) Under-defined square with 0.95 coherence between like axis and with max performance haystack spectrum for all controls	x_1, x_3, y_1, y_3, z_1, z_3
3) Under-defined square with 0.95 coherence between like axis, nearly pure X, and with max performance haystack spectrum	x_1, x_3, y_1, y_3, z_1, z_3
4) Optimal Square control with pure X,Y, & Z that are uncorrelated and with max performance haystack spectrum	x_1, y_1, z_1, y_2, z_2, z_3
5) Optimal Square control with pure roll & yaw that are uncorrelated and with max performance haystack spectrum	x_1, y_1, z_1, y_2, z_2, z_3
6) Optimal Square control with pure X, Y, and Z that are uncorrelated and with respective 810G spectra for X, Y, & Z	x_1, y_1, z_1, y_2, z_2, z_3
7) Rectangular control with pure X, Y, and Z that are uncorrelated and with respective 810G spectra for X, Y, & Z	x_1, y_1, z_1, y_2, z_2, z_3, x_2, x_3, y_3, x_4, y_4, and z_4
8) I/O Transformation control with pure X, Y, and Z that are	x_1, y_1, z_1, y_2, z_2, z_3, x_2,

uncorrelated and with max performance haystack spectrum	x_3, y_3, x_4, y_4, and z_4
9) I/O Transformation control with pure X, Y, and Z that are uncorrelated and with respective 810G spectra for X, Y, & Z	x_1, y_1, z_1, y_2, z_2, z_3, x_2, x_3, y_3, x_4, y_4, and z_4

Table 1: Test types that were performed

The following table summarizes the channel assignment for the various tests:

ADC channel number	Tests 1) to 3) Accels.	Tests 4) to 8) Accels.
1	x_1	x_1
2	x_3	y_1
3	y_1	z_1
4	y_3	y_2
5	z_1	z_2
6	z_3	z_3
7	x_2	x_2
8	y_2	x_3
9	z_2	y_3
10	x_4	x_4
11	y_4	y_4
12	z_4	z_4

Table 2: Channels assignments for the various tests that were performed

In the following, the rest results of all, but test 5), will be discussed. It won't be discussed in the interest of brevity, since its results are similar to those of test 3).

1) Under-defined square control, with zero coherence between control channels and with max performance haystack spectrum

The results shown in the following Fig. 2 were obtained with controls: x_1, x_3, y_1, y_3, z_1, z_3 and auxiliaries: x_2, y_2, z_2, x_4, y_4, z_4, with the input channel assignments that are shown in Table 2. Fig. 2's top plot shows PSDs for x_1, x_3, x_2, and x_4; its middle plot shows them for y_1, y_3, y_2, and y_4; and its bottom plot shows them for z_1, z_3, z_2, and z_4. Note that in the lower plot, the PSDs for z_2 and z_4, which are on the uncontrolled corners 2 & 4, are quite different than what we see in the Z responses for corners 1 and 3, which are being controlled. Thus, the lower plot shows the presence of uncontrolled roll and pitch motions, as one would expect given the fact that the control accelerometers cannot distinguish between roll and pitch.

This means that by controlling only corners 1 and 3, we are not able to uniquely control both roll pitch. This is the probable cause of the uncontrolled roll and pitch on the top face of the cube. This is demonstrated clearly in the lower plot, as one would expect. Because of this, this configuration is not recommended, unless the field data requires it. However, we discuss it to illustrate how accelerometer placement affects the type of motions that are controllable.

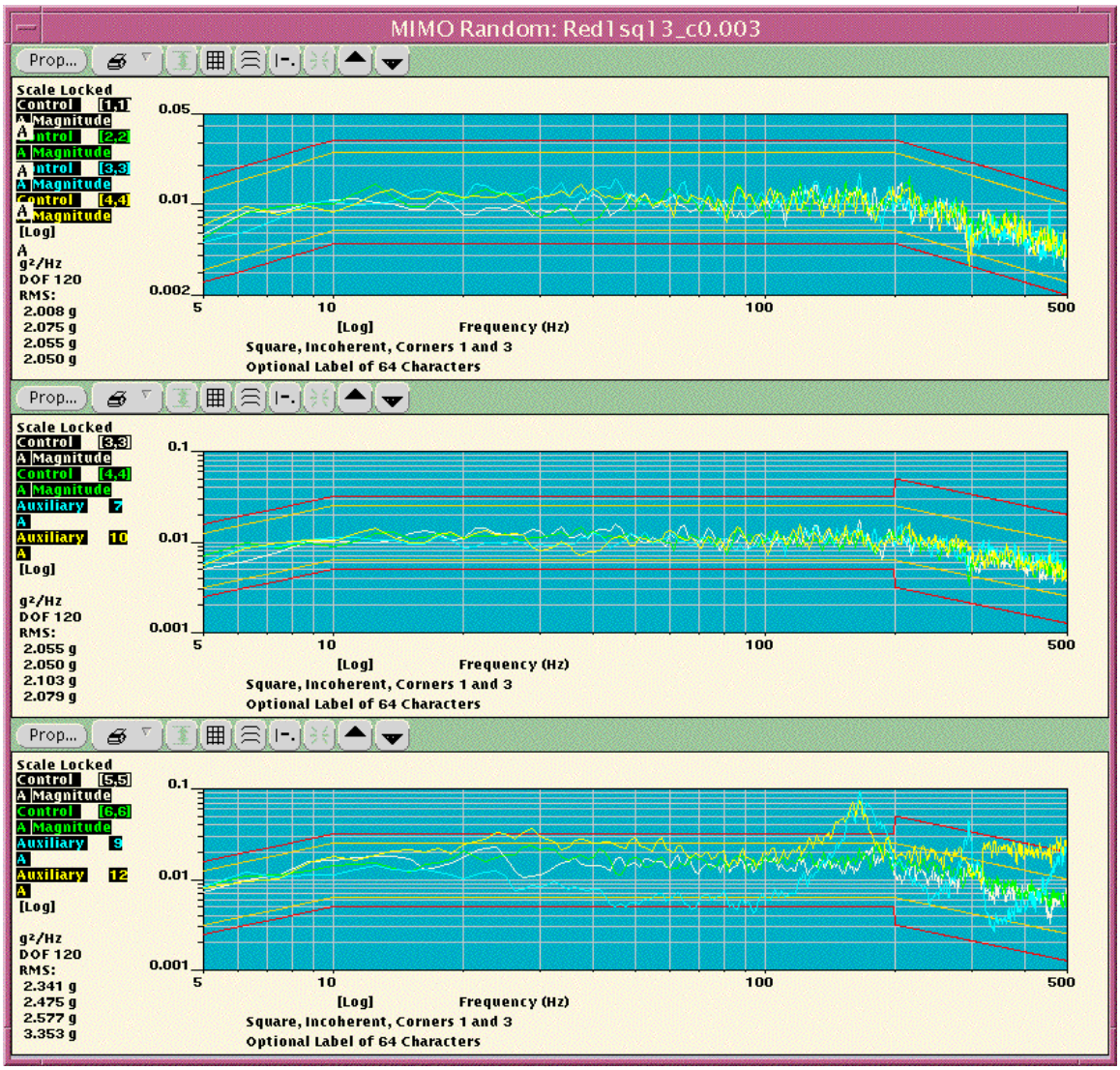

Fig 2: Under defined Square Control with Incoherent Control Responses Specified.

The following Fig. 3 shows the results that were obtained in controlling the relative coherence[1,6] between control channels, with controls: x_1, x_3, y_1, y_3, z_1, z_3 and auxiliaries: x_2, y_2, z_2, x_4, y_4, z_4. In this test, another control goal is for the coherence to be nearly zero between all control channels. Fig. 3's plots show that this goal was largely achieved, even though we don't have an optimal control accelerometer arrangement. This result demonstrates that Cube is capable of being controlled to create 6 independent motions,[6,10] irregardless of whether they are kinematically correct or not in the 6-DOF sense.

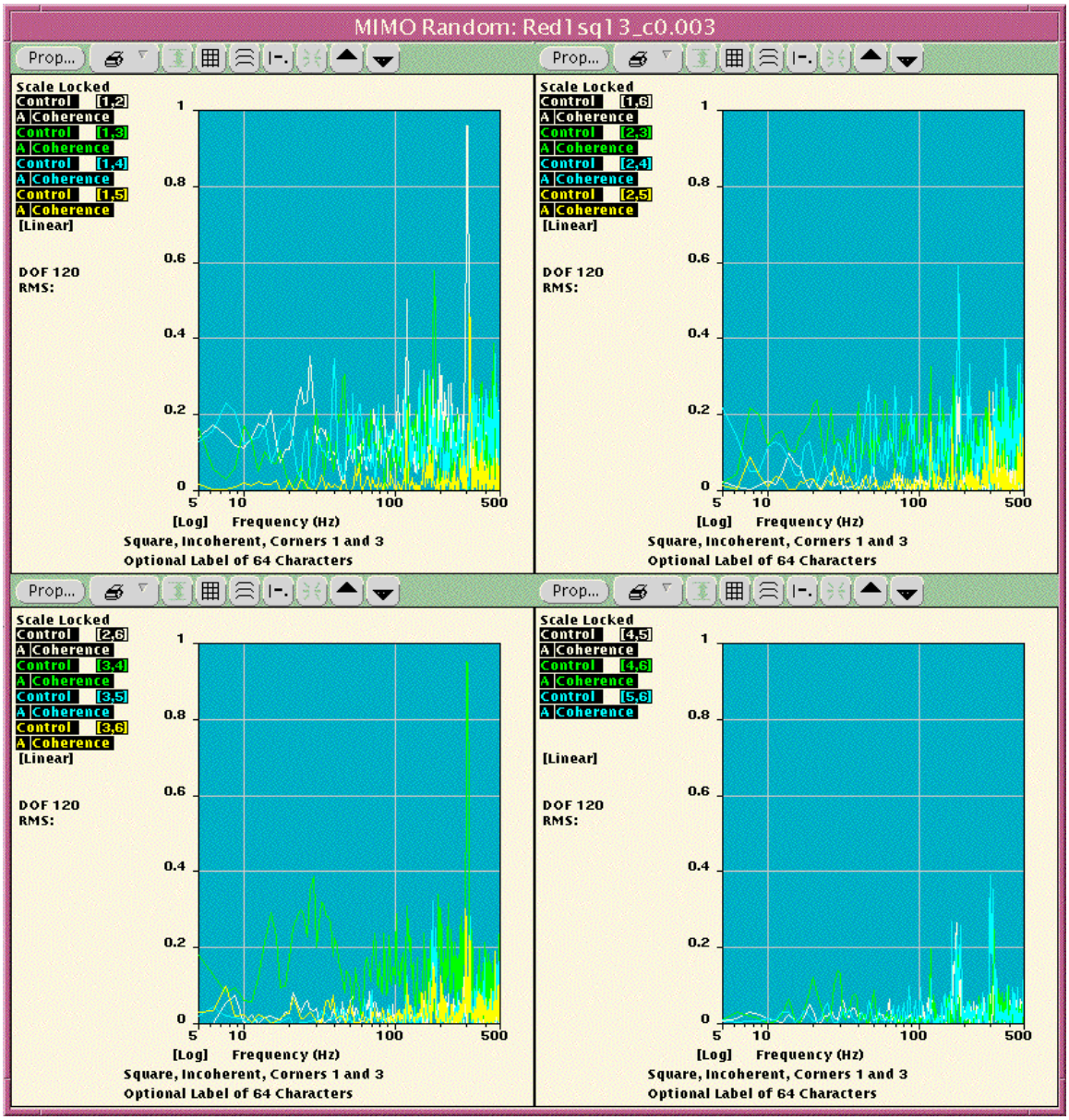

Fig 3: Results of Controlling to Zero Coherence with Under defined Square Control

The fact that the coherence between all control channels is mostly zero, as shown by Fig. 3, indicates that the corners 1 and 3 of the cube are moving as independent points in space.[6] The only significant exception is around 300 Hz, where the coherence between y_1 and z_1 and between x_1 and x_3 is nearly 1, which is indicative of common noise or uncontrolled response on both of these pairs of control responses.[7] The coherence around 185 Hz also has a response on the order of 0.37 or less for many pairs of control channels, which again is indicative of a common, non control related source of vibration[7] like the pedestal resonances in the Cube's actuator supports, which will be further discussed with regards to other presented test data. However, the results indicate that the Cube is capable of having the response two of its corners controlled such that the resultant random responses, in each axis, are statistically independent of each other.[6]

Fig. 4 shows the diagonal elements of both the Drive's SDM[1] and the system-under-test's Impedance Matrix.[1] Note their similarity. Peaks in the respective element spectra correspond to structural anti-resonance frequencies; frequencies at which the Cube is inefficient, by requiring additional drive amplitude in order to maintain a flat response.[1,8] Note that these peaks occur at around 185 Hz and 300 Hz, which are the frequencies at which coherence control was the poorest. This illustrates how peaks in the Impedance Matrix indicate frequencies at which the system-under-test will present control challenges.[1,8] These control challenges affect the achievable accuracy of coherence, phase, and amplitude control, and in that order,[1,8] as these and following results show.

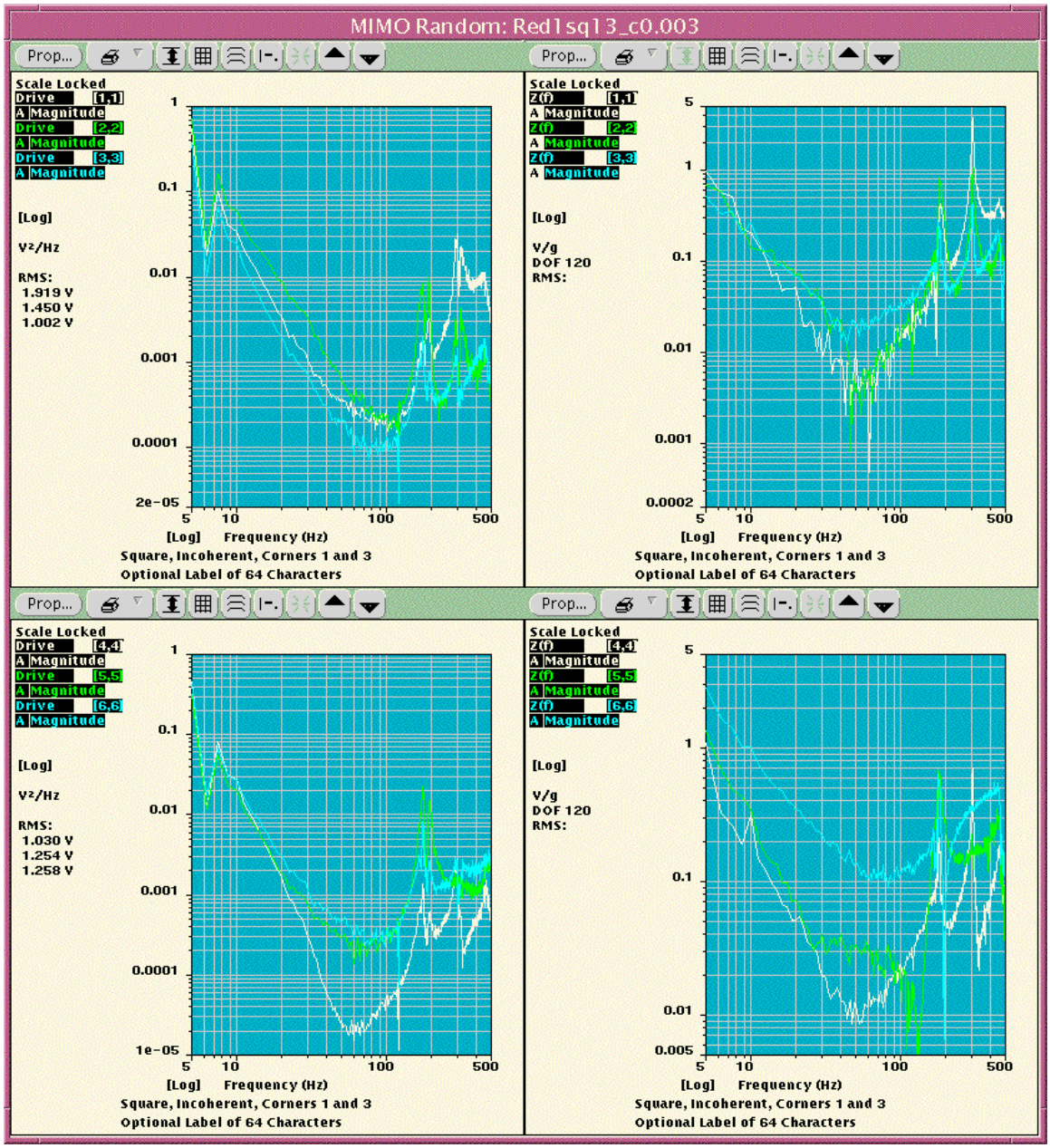

Fig 4: Drive and Impedance Matrices for Under-Defined Square Control

2) Under-defined square control, at control locations 1 and 3, but with 0.95 coherence between pairs of X, Y, and Z responses and with max performance haystack spectrum.

This test is instrumented the same as test 1) with controls: x_1, x_3, y_1, y_3, z_1, z_3, and with auxiliaries: x_2, y_2, z_2, x_4, y_4, z_4. The goal of this test was to cause the top surface of the Cube to move only rectilinearly with no rotations, with the axes incoherent with each other. To accomplish this, the target of the control was to create the same PSD in each axis, but have the axes be uncorrelated with each other, where the same axis responses were specified to have 0.95 relative coherence with each other. The resulting motion of the center of Cube's top surface should then describe a sphere of motion according to Gaussian distribution in 3-space.[6]

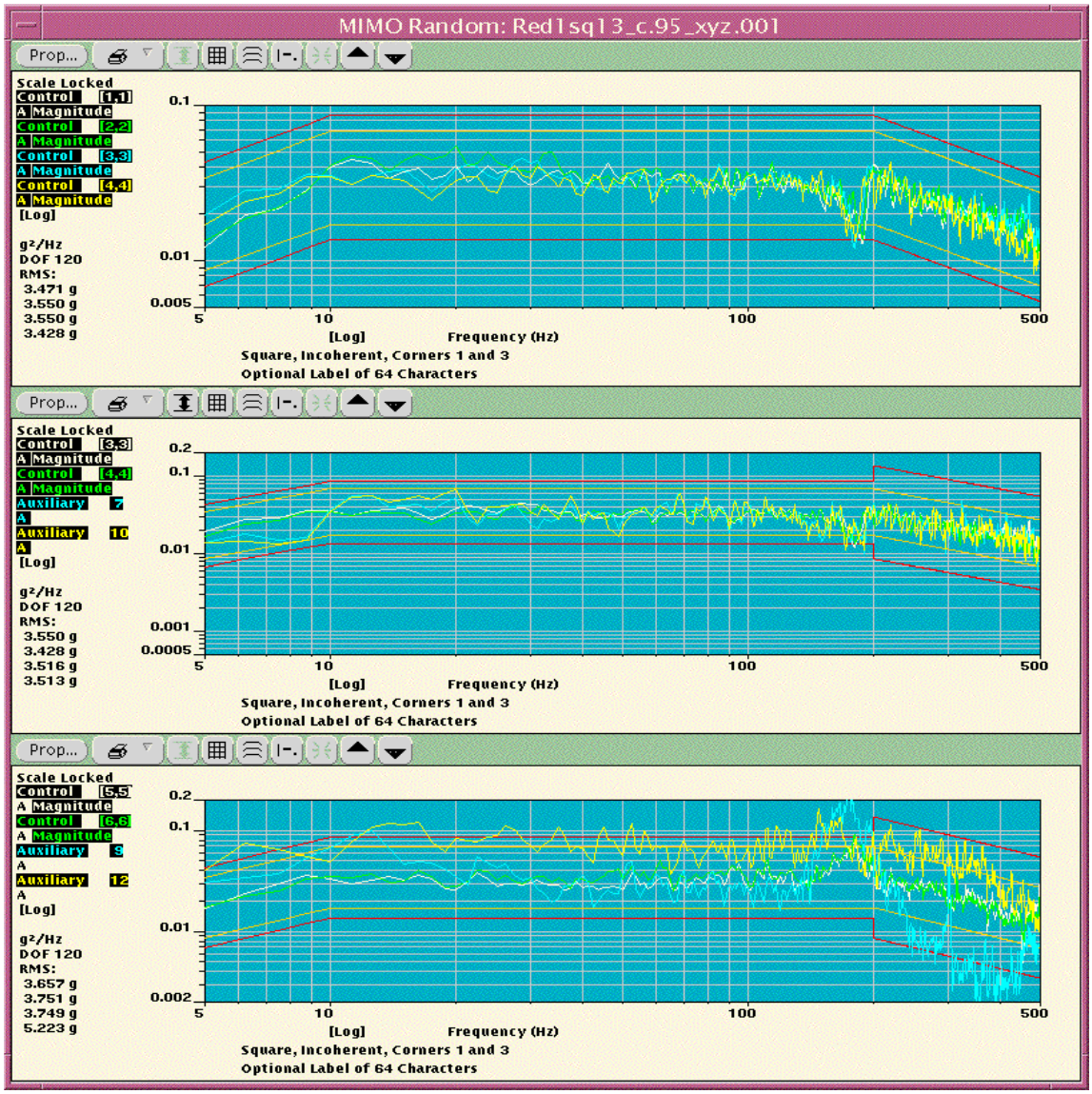

Fig 5: PSD Responses for Auxiliary and Control Accelerometers for Test 2

Fig. 5, like Fig. 2, shows the PSDs of x_1, x_2, x_3, and x_4 in its top plot; the PSDs of y_1, y_2, y_3, and y_4 in its middle plot; and the PSDs of z_1, z_2, z_3, and z_4 in its bottom plot. Note that the PSDs of z_2 and z_4, which are on the uncontrolled corners 2 and 4, are again quite different than what we see in the Z responses for corners 1 and 3, which are being controlled. This again shows the presence of uncontrolled pitch motions as in Fig. 2, which indicates that the goal of no rotations was not met. This again indicates the weakness of this control accelerometer configuration,[3] which can't easily distinguish between roll and pitch, which leads to the aforementioned control problems, as was discussed for the previous test. However, it is more pronounced in this case and with more control difficulties in the area of 185 Hz. The problems at 185 Hz will be described more later, but this test is more difficult than Test 1, since commanding high coherence between like axis control points requires more power, which exacerbates the lack of uniformity that we saw in the previous test, which probably results in more undesirable rotations about X and Y.

However, the main point again is that by controlling only corners 1 and 3, we are not able to uniquely control both roll and pitch, which is probably the most significant cause of the excessive roll and pitch motions on the top face of the cube. This is exacerbated by the larger power demands of suppressing rotations, which is associated with the high coherence achieved between like axis control responses, as shown in the following Fig. 6.

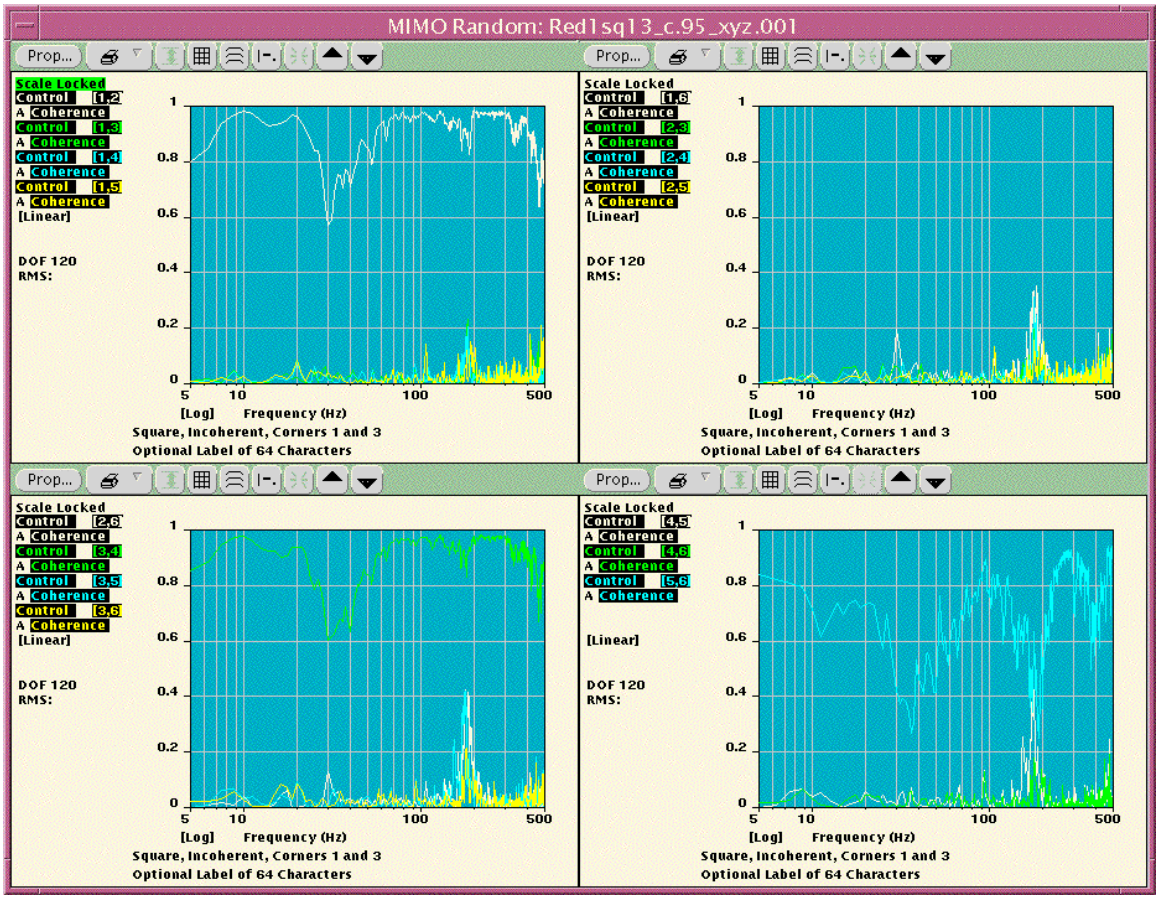

Fig 6: Coherence Response Between Control Accelerometers for Test 2

For test 2), the additional objective was to control the coherence between x_1 and x_3; y_1 and y_3; and z_1 and z_3 to be 0.95, with the coherence zero between different axes, and with all PSD responses to be the same as in the last test and as shown in Fig. 5. Fig. 6 shows the coherence results that were obtained for this test. Fig 6 shows the coherence between x_1 and x_3 in the upper left corner, the coherence between y_1 and y_3 in the lower left hand corner, and the coherence between z_1 and z_3 in the lower right hand corner. The other plots and traces show some of the other coherence spectra that were achieved between different axes responses, which are nearly zero. Thus, these plots show that the coherence goals were largely met, but with significant incoherent responses with other like axis accelerometers on the uncontrolled corners 2 and 4.

Fig 7: Phase Response Between Like Axis Control Accelerometers for Test 2

Fig. 7 shows that the relative phase responses between like axis responses were held near zero phase, with the worst case error on the order of 20^o near 185 Hz, which will later be further discussed. This indicates that if the accelerometers were better placed, we would have achieved pure rectilinear motion. This shows how important accelerometer placement is to a successful MIMO vibration test.

3**) Under-defined square with 0.95 coherence, with: nearly Pure X response, max performance haystack spectrum, and with controls: x_1, x_3, y_1, y_3, z_1, z_3 and auxiliaries: x_2, y_2, z_2, x_4, y_4, z_4.**

The goal of this test was to achieve nearly pure X response with the use of square control, but with a non-optimal control accelerometer configuration. To achieve this, the Y and Z axis control accelerometers were specified to respond with PSD levels one hundredth of the levels that were used for the X axis control accelerometers. Like in test 2) the coherence between like axis control accelerometers was set to 0.95 and their relative phase was set to 0^o, between the respective X and Y axis control accelerometers, but with 180^o between the Z axis accelerometers.

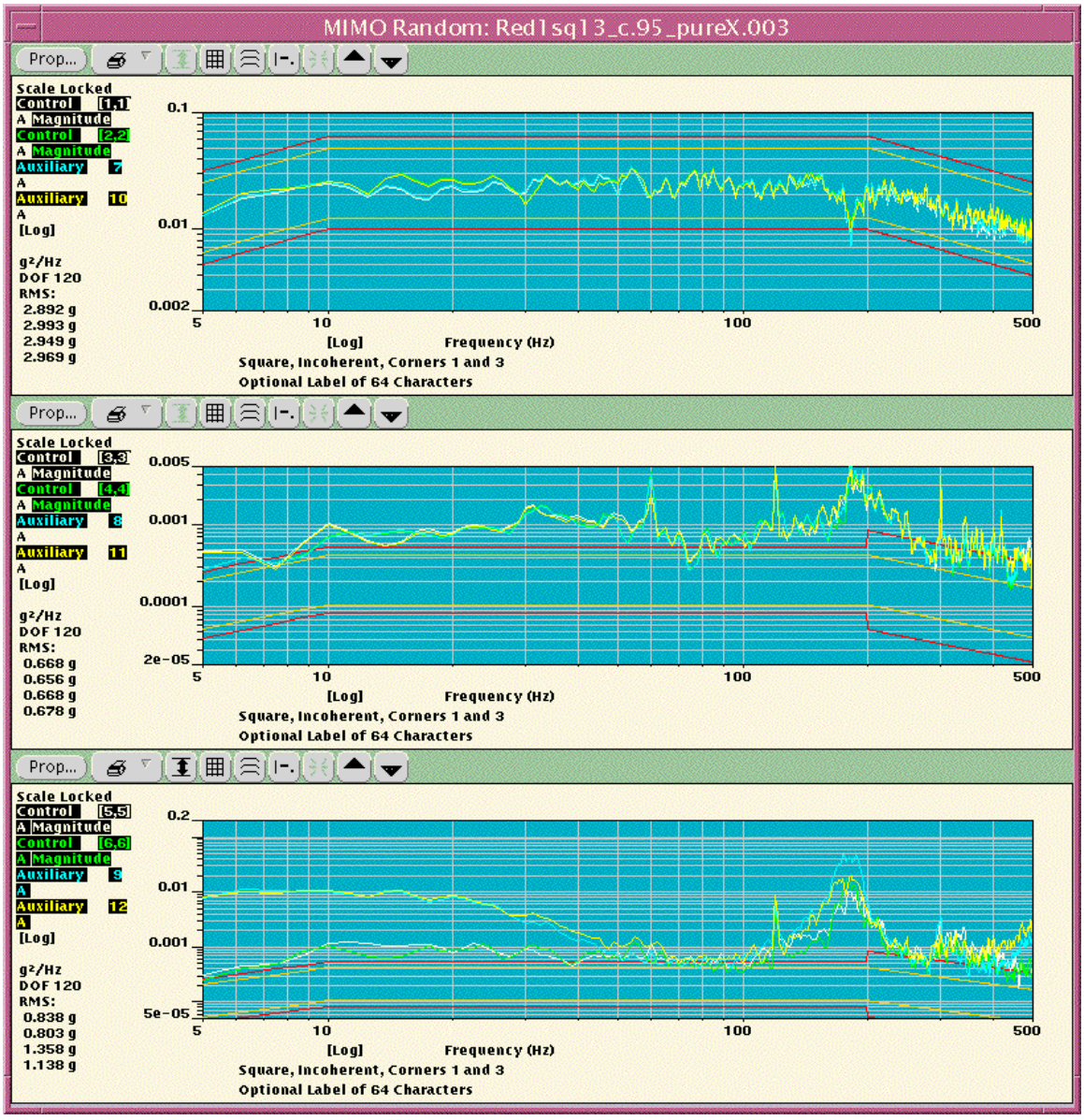

Fig 8: PSD Responses for Auxiliary and Control Accelerometers for Test 3

The previous Fig. 8 shows the PSDs for both the control and auxiliary accelerometers that were achieved. Fig. 8's top plot shows the response PSDs for accelerometers: x_1, x_3, x_2, and x_4; its middle plot shows them for y_1, y_3, y_2, and y_4; and its bottom plot shows them for z_1, z_3, z_2, and z_4. Note that in this case, all of the Y and Z accelerometer responses are quite similar, but that z_2 and z_4, which are on corners 2 and 4 and are uncontrolled, are again quite different than what we see in the Z- responses for corners 1 and 3, which are being controlled. However, within the limits of the test accelerometer's noise floor, we are able to attenuate the Y and Z responses by about a factor 4 with respect to the X response, which results in almost pure X motion to the eye. Test 3) provides an example of how to suppress unwanted DOFs with respect to the principal X DOF, without the use of I/O transformations. How well this works is limited by the instrumentation and actuation noise floors as Fig. 8 amply shows.

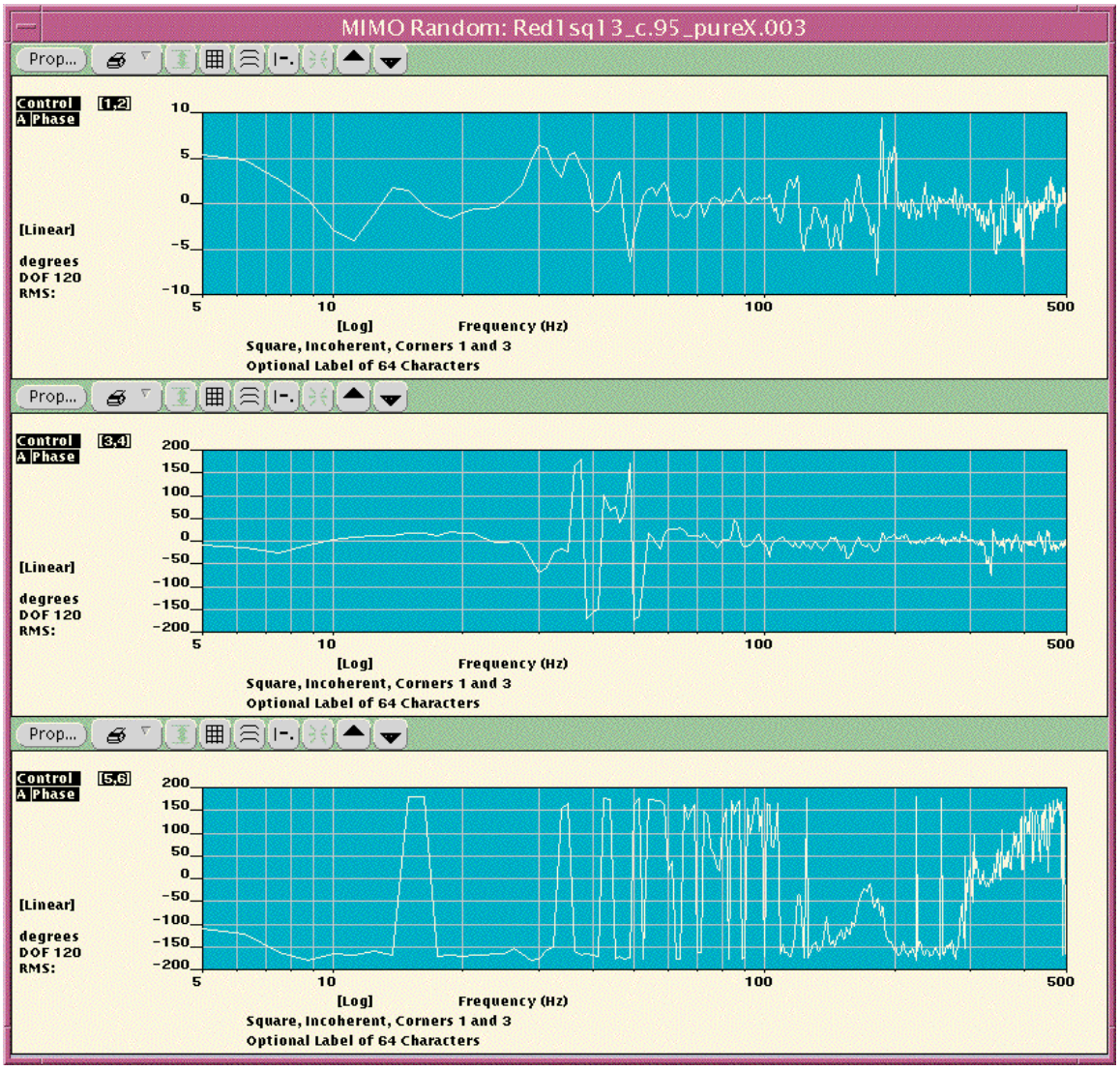

Fig. 9: Phase Response Between Like Axis Control Accelerometers for Test 3

As in the previous two tests, by controlling only corners 1 and 3, we are not able to uniquely control both roll pitch, which is the probable cause of the lack of uniform motion on the top face of the cube, which manifests itself in the discrepancies we see in the response of z_2 and z_4 on the uncontrolled corners 2 and 4, which again indicate uncontrolled roll and pitch. However, since the Z responses are low with respect to the X axis levels, this roll and pitch motion is not visible to eye, as it was in tests 1) and 2).

The previous Fig. 9 shows the relative phase response results that were obtained. It is constructed similarly to Fig. 7. As was discussed previously, in this test, we commanded a 0.95 coherence between like axis responses and zero phase response between x_1 and x_3; between y_1 and y_3; and 180^o phase response between z_1 and z_3. The Fig. 9's plots show that this control goal was largely met. However, if the goal is to control 6-DOF motions, this accelerometer arrangement is not recommended, since roll and pitch cannot be separately controlled, as the data from the three tests we've described amply show.

4) Optimal Square control that uses x_1, y_1, z_1, y_2, z_2, and z_3 for control, with 0.95 coherence between the two y accelerometer's and between the three z accelerometer's responses (pure X, Y, Z uncorrelated).

As we've discussed, the under-defined square control methodology is not recommended for 6-DOF motion control. It suffers from the fact that it does not adequately describe roll and pitch motions. A better instrumentation choice is that of optimal square control. In this case, the control accelerometers are arranged so that the Z accelerometer locations define a plane, vs. defining a line as in the under-defined case. In this case, we use the 3 tri-axial accelerometers that are located on corners 1, 2, and 3 of the Cube, as shown in Fig. 1. This configuration is called optimal, because this control accelerometer arrangement gives enough information to uniquely determine both roll and pitch,[3] and thus all of the 6 rigid-body DOFs of the top surface of the Cube, with only 6 such control accelerometers. In later sections we will explore what happens when we use more than 6 control accelerometers.

Fig. 10 shows the PSD results that were obtained for test 4). Its top plot shows the response PSDs for accelerometers x_1, x_2, x_3, and x_4; its middle plot shows the same for y_1, y_2, y_3, and y_4; and its bottom plot shows the response PSDs for z_1, z_2, z_3, and z_4. Note that in this case, all of the X, Y and Z accelerometer responses are quite similar, but that x_2, x_3 and x_4, which are uncontrolled, are quite different around 185 Hz from what we see in the x_1- response, which is being controlled. These results indicate that the top surface of the cube moves much more uniformly, probably due to the more optimal arrangement of control accelerometers. To the eye it looks like pure X, Y, and Z motions with no noticeable roll, pitch, and yaw motions.

This configuration, although optimal in the sense that it can be used to describe the 6-DOF motion of the top surface of the cube, uses an unequal number of accelerometers for each axis: 1 for X, 2 for Y, and 3 for Z. To further complicate matters, the cube is more difficult to control around 180-185 Hz, due to internal design factors, which are a result of resonance of the pedestals that support the vertical axis actuators. (Note that Team has

a cast base option that pushes the problem at 180-185 Hz to nearly 500 Hz, which we did not use.) Additionally, in this case, since we're preventing rotations more effectively, more power is required from the Cube. Thus, these three factors are probably what are responsible for the one discrepancy we see around 180-185 Hz, by further exciting the pedestal resonance. Otherwise, these PSD results indicate that the optimal square control methodology is an effective way to accomplish 6-DOF testing with the Cube.

Fig. 10: PSD Responses for Auxiliary and Control Accelerometers for Test 4

In the following Fig. 11, we show the coherence results that were obtained with this optimal accelerometer configuration. These coherence results show that the coherence between y_1 and y_2 and between z_2 and z_3 was largely at 0.95, as commanded. The other, inter-axis coherences, were largely near zero, also as commanded. The only area of significant control error was near 185 Hz, which is a problem frequency for the cube near it maximum performance demands, as was discussed previously. We will see in later results that the performance near the Cube's problem frequency improves with more

sophisticated control methodologies and a more uniform control accelerometer placement.

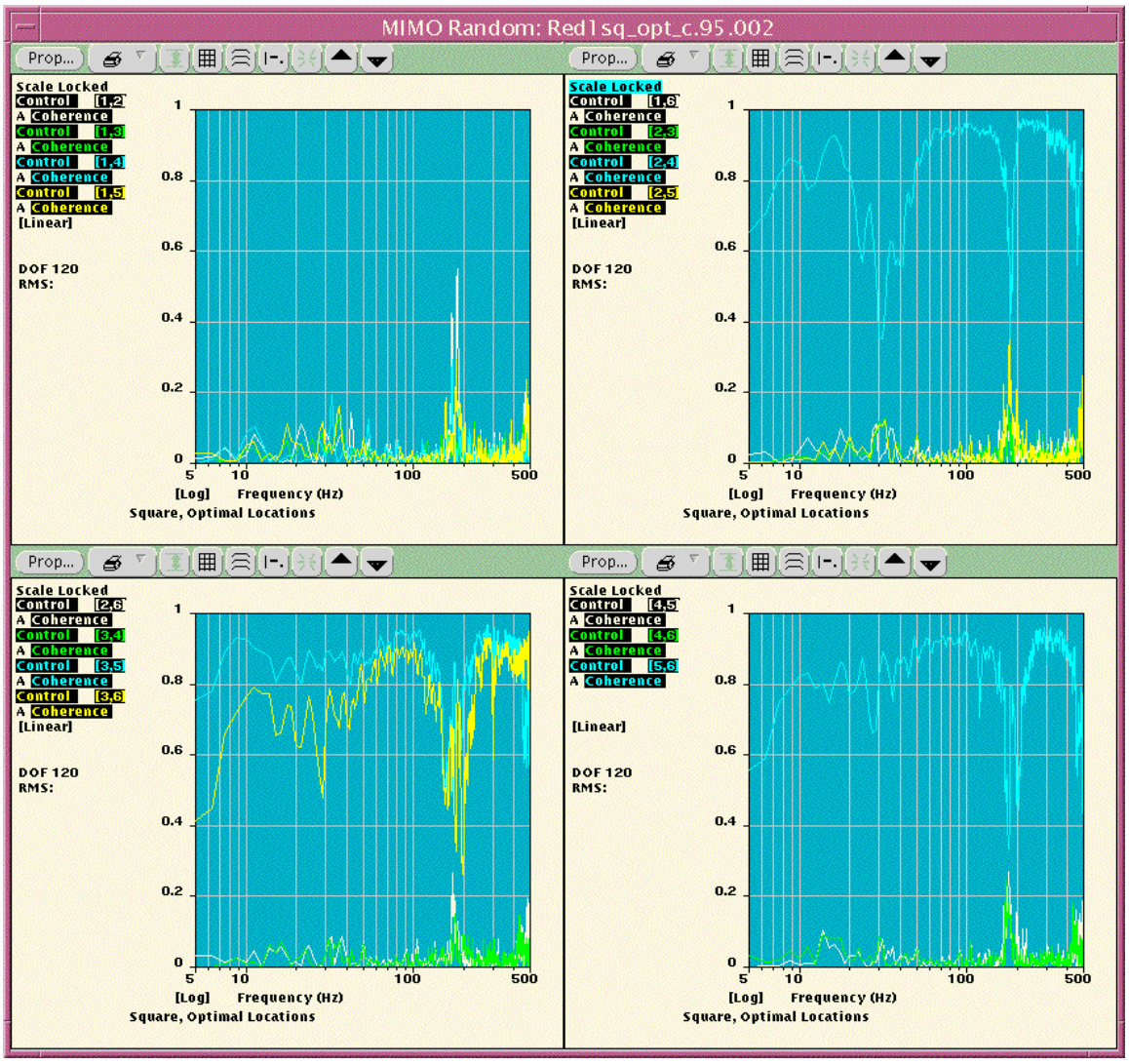

Fig. 11: Coherence Response Between Control Accelerometers for Test 4

The following Fig. 12 shows the relative phase response results that were obtained for test 4). Fig. 12 is constructed similarly to Figs. 7 and 9. As was discussed previously; in this test, we commanded a 0.95 coherence between like axis responses and 0^o phase response between y_1 and y_2 and 0^o phase response between z_1, z_2 and z_3. Fig. 12's plots show that this control goal was largely met. Thus the results that Figs. 11 and 12 show, validate what one sees with one's eyes, i.e. pure rectilinear motion in X, Y, and Z, which describes a sphere in space, as one would expect.[6]

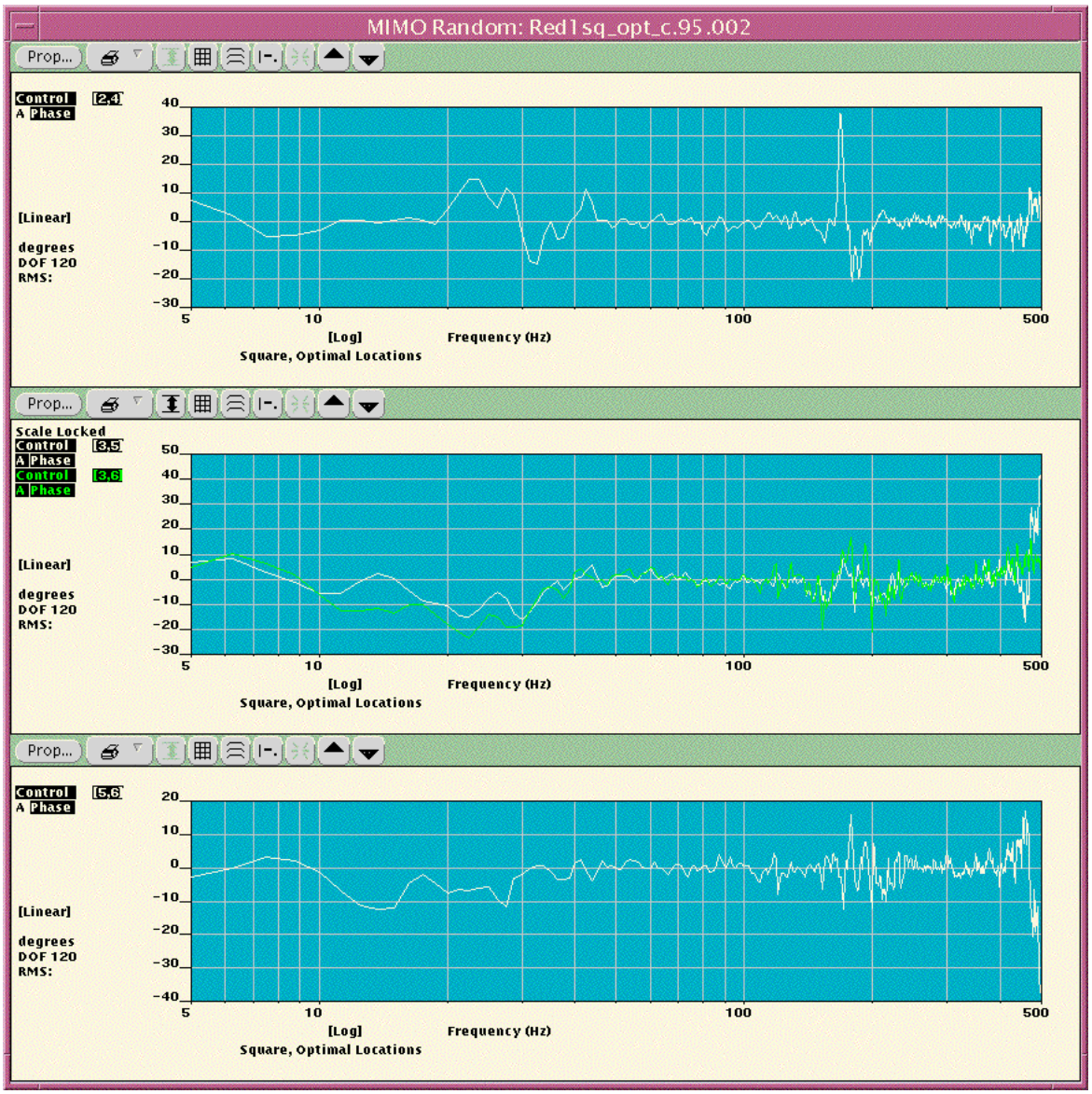

Fig. 12: Phase Response Between Like Axis Control Accelerometers for Test 4

6) Optimal Square control with pure X, Y, and Z, which are uncorrelated, using 810G spectra, with controls: x_1, y_1, z_1, y_2, z_2, z_3, and auxiliaries: x_2, x_3, y_3, x_4, y_4, z_4.

These are the same conditions as in test 4), but with the respective X, Y, and Z axis set to use the 810G spectra instead of the maximum performance haystack spectrum. The following Fig. 13 shows the PSD results we obtained from the 12 tri-axial accelerometers that have been used in the testing heretofore. Again, its top plot shows the X-axis accelerometer responses, its middle plot shows the Y-axis accelerometer responses, and its bottom plot shows the Z-axis accelerometers responses.

Fig. 13's plots show that all of the same axis accelerometer responses match very well. It also shows excellent control performance for this reduced level of the 810G test, but with all axes tested simultaneously.

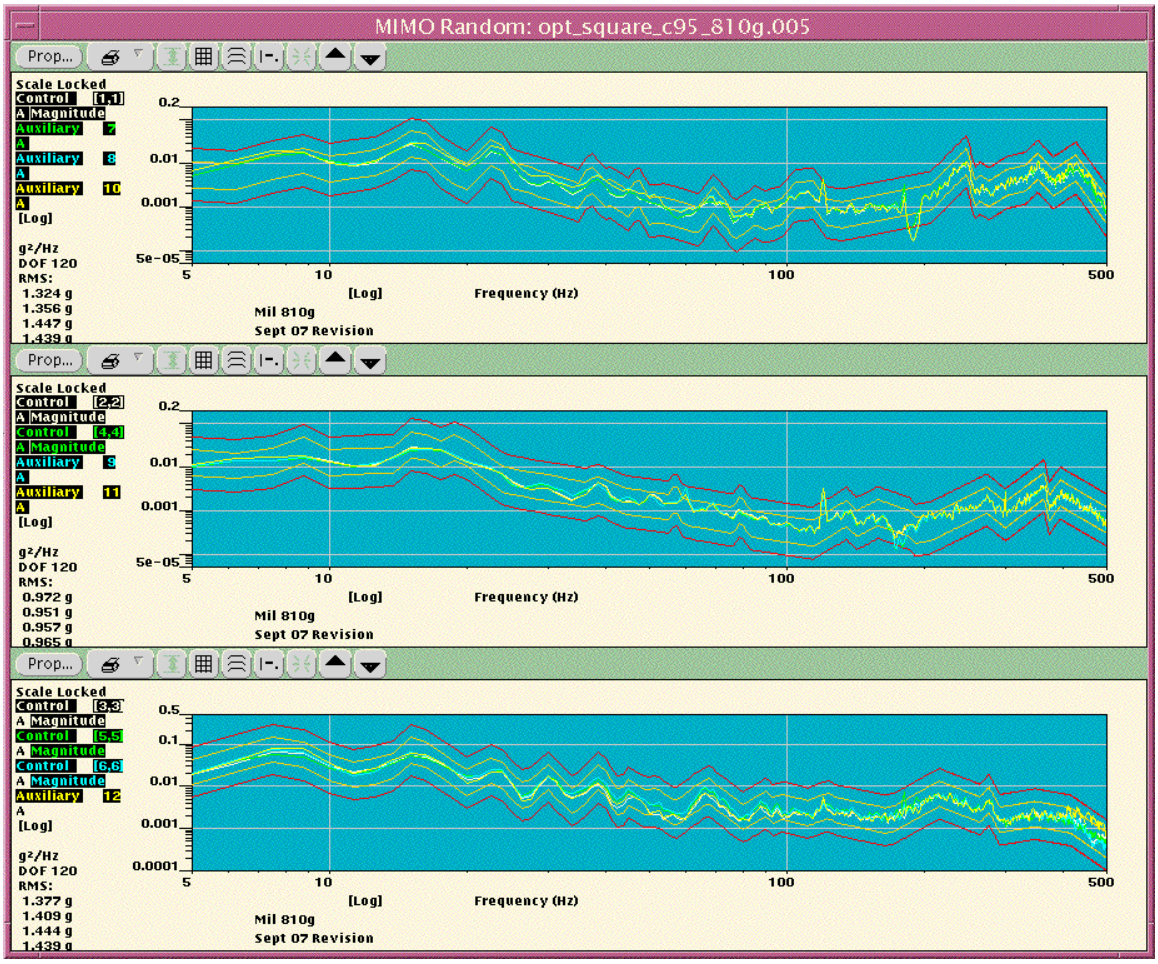

Fig. 13: PSD Responses for Auxiliary and Control Accelerometers for Test 6

The only trouble spots are the familiar 185 Hz problem and around 120 Hz, due to the relatively low level of the acceleration response around the power harmonic frequency. Additionally, we found that we needed to limit the low frequency energy to be able to run the 810G test at full level. It's felt that if 3-sigma clipping were enabled, this would also allow this test to be run at full level. However, the controller has this function disabled at this time, because experience in the field has shown that an over zealous use of sigma-clipping causes a reduction in control dynamic range. However, more testing is planned to test to see if relaxing this constraint would result in being able to run this test at full level without having to compromise at the lowest frequencies.

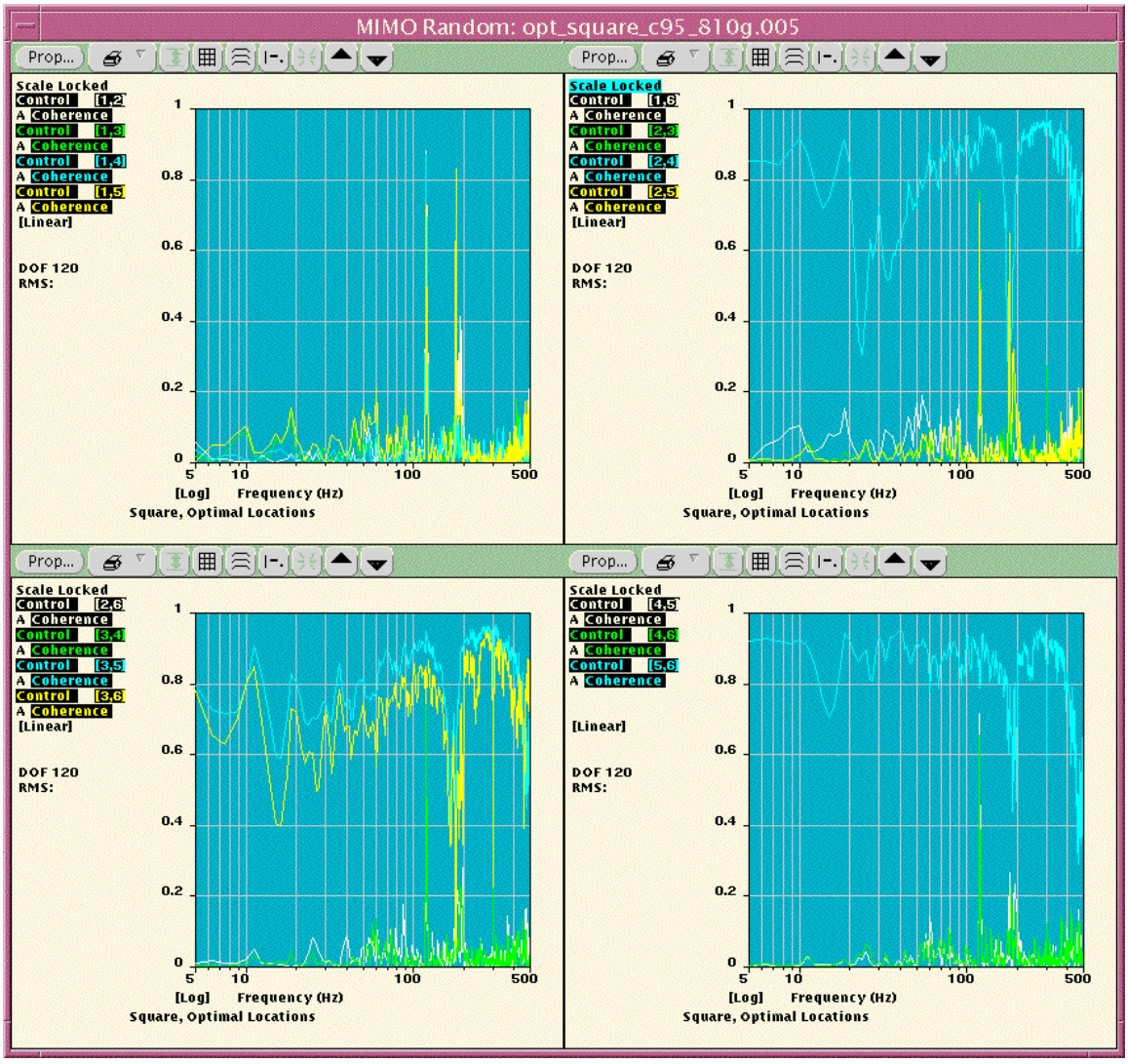

Fig. 14: Coherence Response Between Control Accelerometers for Test 6

In Fig. 14, we show the coherence results that were obtained with this optimal accelerometer configuration and the 810G test specifications. These coherence results show that the coherence between y_1 and y_2 and between z_1, z_2 and z_3 was largely at 0.95, as commanded and as in test 4). The other, inter-axis coherences, were largely near zero, also as commanded, as in test 4). The only area of significant control error was again near 185 Hz, as was discussed previously.

The relative phase response results that were obtained, were also quite similar to what was obtained for test 4) and will not be shown, in interest of brevity. Also, to the eye, the Cube was moving in pure rectilinear motion, as in test 4), which again validates the use of the optimal 6 accelerometer placement of tests 4) and 5) for 6-DOF testing, which is recommended for general use, if available control accelerometers are limited in number.

However, if control accelerometers are not so limited in number, the next test results we discuss show that there is an advantage to using over-determined control strategies.

Over Determined Control

Thus, the use of over determined control was investigated next to see if it improves the results that have been obtained for tests 1), 2), 3), 4), and 6) that have been previously discussed. Over determined control occurs whenever there are more control accelerometers and/or actuators than controlled DOFs. Two approaches can be used: Rectangular Control or I/O Transformation Control. Rectangular Control uses the Moore-Penrose Pseudo-Inverse[1] of the Frequency Response Matrix, which describes the dynamics of the system-under-test,[1,4] for control to achieve least squares control.[4] I/O Transformation uses the known linear dependence between input signals and/or the multiple actuators to make the Frequency Response Matrix used for control be full-rank.[1,5] The use of both of these advanced control methods were then investigated in the next sequence of tests.

7) Rectangular control with pure X, Y, and Z, which are uncorrelated, using 810G spectra, and with controls: x_1, y_1, z_1, y_2, z_2, z_3, x_2, x_3, y_3, x_4, y_4, z_4.

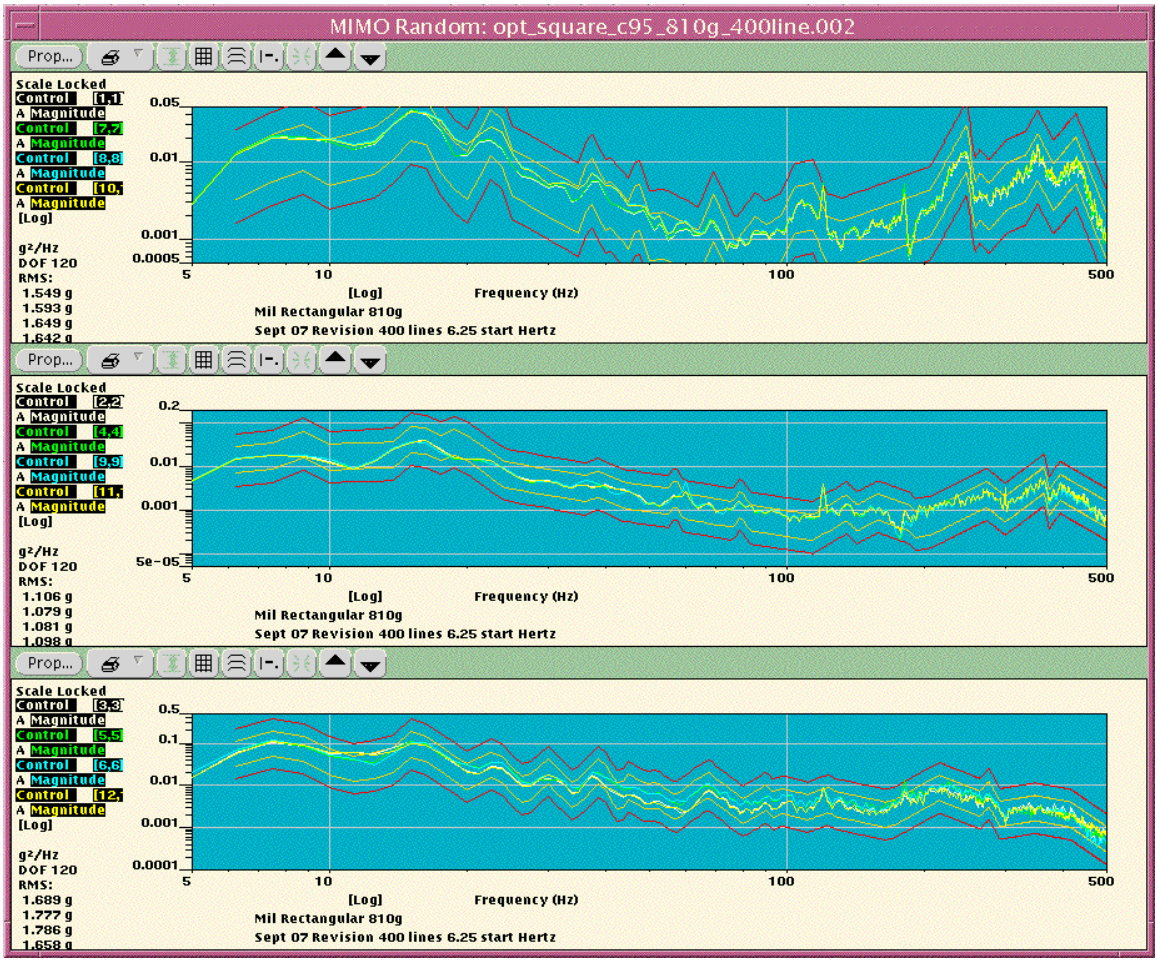

Fig. 15: PSD Responses for Control Accelerometers for Test 7

This test makes all 4 tri-axial accelerometers control accelerometers, for a total of 12 control accelerometers. In this case, the control SDM[1,4] is a 12x12 matrix. Fig. 15 shows the PSD responses we obtained for control channels: x_1, y_1, z_1, y_2, z_2, z_3, x_2, x_3, y_3, x_4, y_4, z_4. Notice that all of the same axis responses are now more similar to each other than they were for test 6). This is probably due to the fact that they are now all under control and that the control accelerometer configuration is now more uniform, where we now have 4 control accelerometers for each rectilinear axis. The one significant result of Fig. 15 is that it shows that the performance at 185 Hz is also improved, relative to the last case, which validates that this a better control methodology than the optimal square control methodology of the last sections.

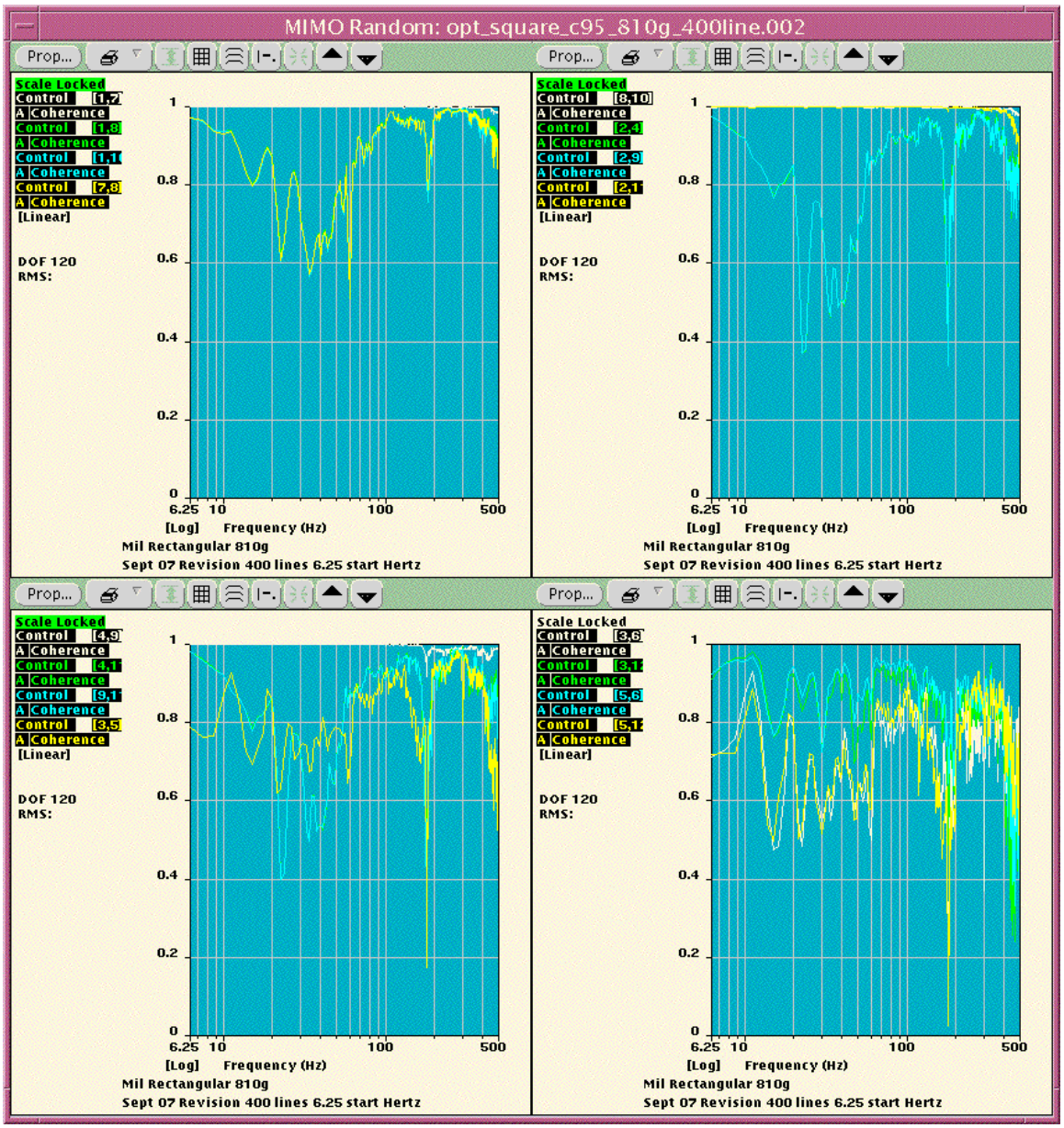

Fig. 16: Coherence Response Between Control Accelerometers for Test 7

Rectangular control typically results in matching the response SDM to reference SDM in the least squares sense, where each response can differ from its respective reference.[4] In this case, we found that the responses all match their respective reference spectra within the test tolerances, as Fig. 15 shows. This indicates that the top surface of the Cube is largely moving as a rigid body. The spikes at 120 and 180 Hz are probably the power line harmonics due the relatively low voltage near those frequencies. In any case, all responses are now within the test abort tolerances, which had not been the case before.

The previous Fig. 16 shows the coherence results that were obtained for like axis control response accelerometers. These results show that the respective X, Y, and Z accelerometers are all nearly coherent. Notice how similar they are to each other and how close they are to the target value of 0.95, with the exception around 185 Hz. Although not shown, the coherence between dissimilar axes, was also found to be around 0.0, as commanded.

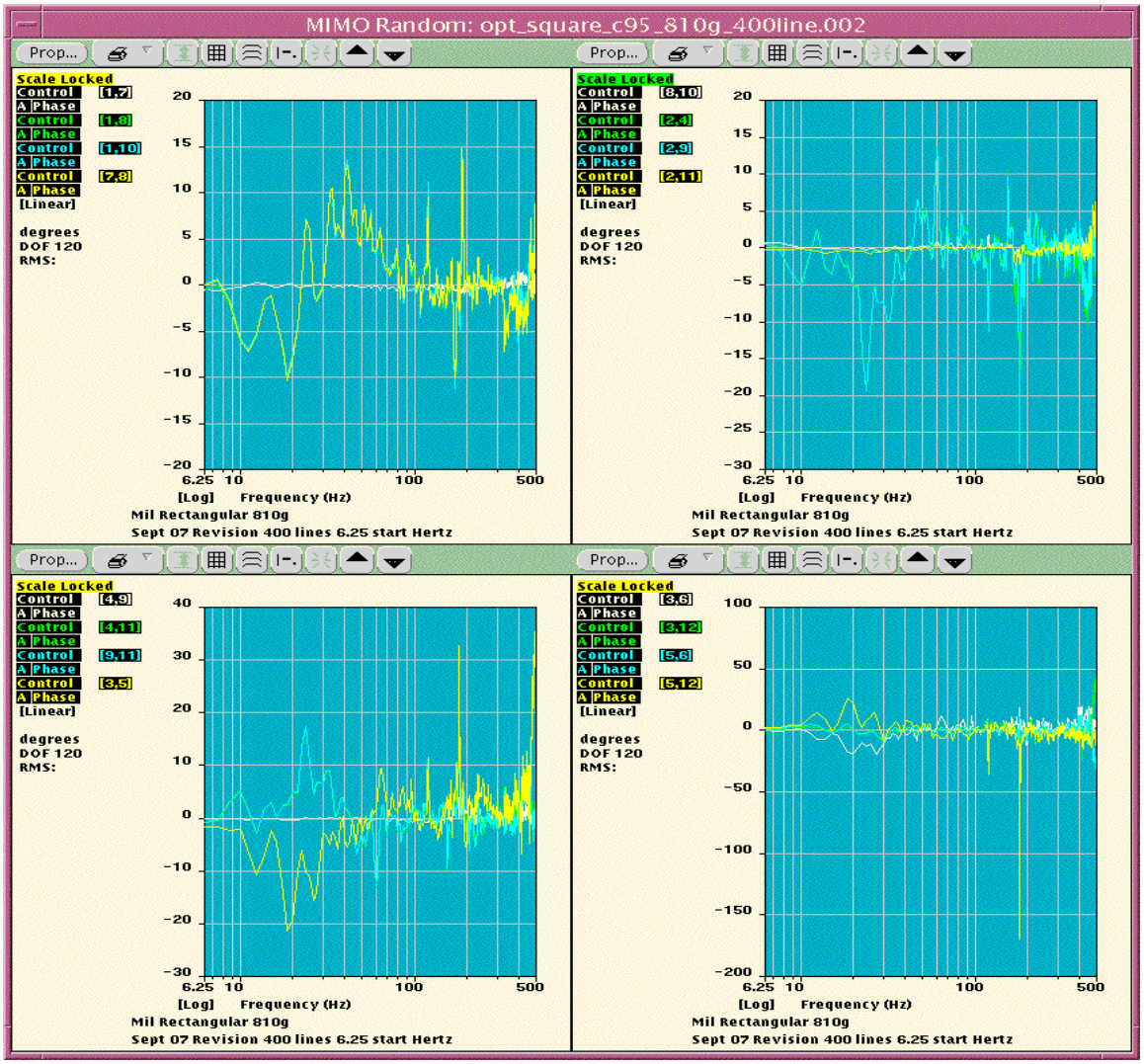

Fig. 17: Coherence Response Between Control Accelerometers for Test 7

The corresponding phase results, which are shown in Fig. 17, also show that the relative phase between like axis control accelerometers are also nearly zero, except at 185 Hz, as has occurred in other tests.

These three plots show that the use of rectangular control results in a more uniform motion across the top surface of the Cube and that the axes are uncorrelated, but moving as a rigid body undergoing 3-axes uncorrelated motion with little to no visible rotations.

I/O Transformation Control

For the next two tests we used I/O transformation control. As we've discussed, only an input transformation[9,10] was used to convert the accelerometers signals from actuator space to 6-DOF space. The input transformation that was used is:

$$\begin{Bmatrix} X \\ Y \\ Z \\ R_x \\ R_y \\ R_z \end{Bmatrix} = \begin{bmatrix} 0.25 & 0 & 0 & 0 & 0 & 0 & 0.25 & 0.25 & 0 & 0.25 & 0 & 0 \\ 0 & 0.25 & 0 & 0.25 & 0 & 0 & 0 & 0 & 0.25 & 0 & 0.25 & 0 \\ 0 & 0 & 0.25 & 0 & 0.25 & 0.25 & 0 & 0 & 0 & 0 & 0 & 0.25 \\ 0 & 0 & -6.23 & 0 & -6.23 & 6.23 & 0 & 0 & 0 & 0 & 0 & 6.23 \\ 0 & 0 & 6.23 & 0 & -6.23 & -6.23 & 0 & 0 & 0 & 0 & 0 & 6.23 \\ 3.12 & -3.12 & 0 & 3.12 & 0 & 0 & 3.12 & -3.12 & 3.12 & -3.12 & -3.12 & 0 \end{bmatrix} \begin{Bmatrix} x_1 \\ y_1 \\ z_1 \\ y_2 \\ z_2 \\ z_3 \\ x_2 \\ x_3 \\ y_3 \\ x_4 \\ y_4 \\ z_4 \end{Bmatrix} \quad \text{(Eq. 1)}$$

(Eq. 1) is used to transform the time histories from the input accelerometers into control DOFs. The matrix elements in its bottom three rows have a conversion factor to convert between G's into radian/sec^2. Its determination uses the geometry of the accelerometer placement for its determination.[9,10] For an output transformation,[5,10] we used the Identity Matrix and the Impedance Matrix. This is possible because the Impedance Matrix describes the coupling between actuators and responses, which in particular also includes rigid body coupling, as in the Cube's.[1]

8) I/O Transformation control with pure X, Y, and Z that's uncorrelated with max performance haystack spectrum, and with controls: x_1, y_1, z_1, y_2, z_2, z_3, x_2, x_3, y_3, x_4, y_4, z_4.

In this test and the next, we use the input transformation given by (Eq. 1) to reduce the 12 input control accelerometers into the control DOFs: X, Y, Z, R_x, R_y, and R_z, i.e. the classic 6-DOF rigid-body control responses.[3,5,9,10] The rotations were defined at levels slightly above the instrumentation's noise floor, but with an accentuated low frequency end to cause visible roll, pitch, and yaw motions, which were witnessed.

The following Fig. 18 shows the PSDs associated with the control DOFs and their respective test tolerances. Notice it shows that all controlled axes responses are within

their tolerance bands, except around 185 Hz. We think that this control discrepancy is worse than with rectangular control, because we are now using the Cube's 6-DOF capabilities to cancel unwanted rotational motion and to cause rotations at the lowest frequencies. This requires additional resources, which exacerbates the 185 Hz phenomena, which is an internal resonance that is not directly controllable.[1,8]

Fig. 18: PSD Responses for the Control DOFs for Test 8

Also note that the top plot in Fig. 18 shows the 3 rectilinear responses for X, Y, and Z in G's and that the bottom plot show the 3 rotational responses in rad/sec2, all of which are inside their respective test tolerance except around 185 Hz.

The following Fig. 19 shows the response of the control input accelerometers, before the input transformation. These plots show, the X-input accelerometer responses in the top plot, the Y-input accelerometer responses in the middle plot, and the Z-input accelerometers responses in the bottom plot. Notice how similar the same axis accelerometer responses are to each other. This is expected, since the rotations are small as compared to the translational responses. The only control "problem" is near 185 Hz, also as expected. Note that we're achieving this result with only 6-drives and no output transformation,[5,10] other than what the Impedance matrix provides.

Fig. 19: PSD Responses for the Control Inputs for Test 8

The following Fig. 20 shows the relative coherence between control inputs. The top plot shows the relative coherence between some of the X-axis responses, the middle plot shows the coherence between some of the Y-axis responses, and the bottom plot shows the coherence between the Z-axis responses, which should have high coherence. Note that these coherences are better behaved than what we achieved with rectangular control. Several channel pairs of like axis responses exhibited coherence values that approximate 1.0 to 6 digits, much higher than what is possible with rectangular control. However, the commanded reference spectra are different than what we used for rectangular control.

In the section about test 9), we will discuss the use of I/O transformational control with the 810G profiles, as we did for rectangular control, which will allow the two control methodologies to be more easily compared. However, this test shows the ability to cause rotations and also to suppress rotations, as a function of frequencies, and is a good example of the benefits that are possible with MIMO Random and the use of I/O transformations.

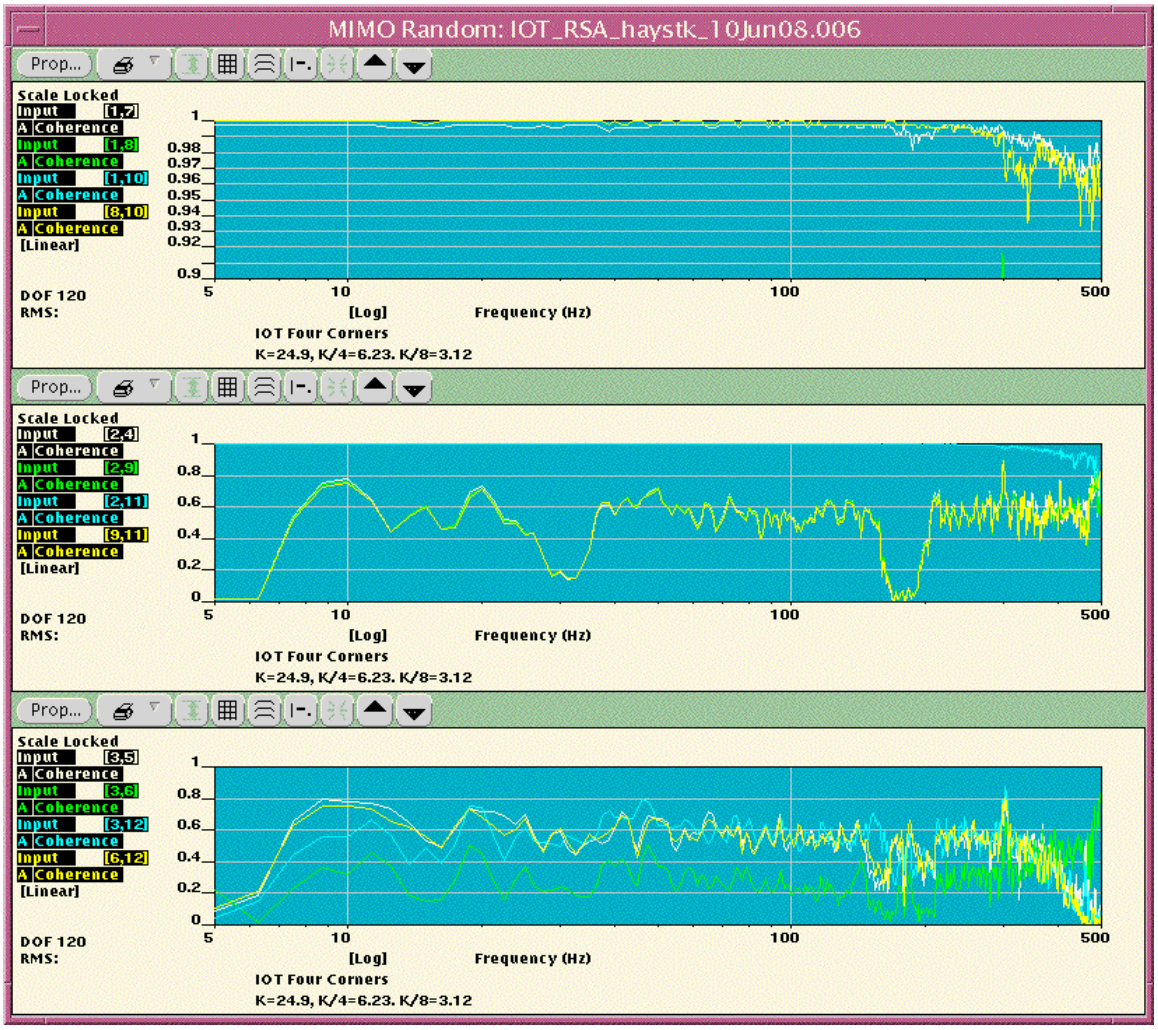

Fig. 20: Selected Coherence Responses Between Control Inputs for Test 8

The following Fig. 21 shows the relative phase response that was achieved for the same control input channel pairs. The top plot shows the relative phase between the same X-axis responses, the middle plot shows the relative phase between the same Y-axis responses, and the bottom plot shows the relative phase between the same Z-axis responses. Note that these relative phases are better behaved than what we achieved with rectangular control.

In any case, we found that the overall test performance does seem better than what we obtained with rectangular control. However, the commanded reference spectra are different than what we used for rectangular control. Thus, in the next test we use the same 810G references that were used for test 7).

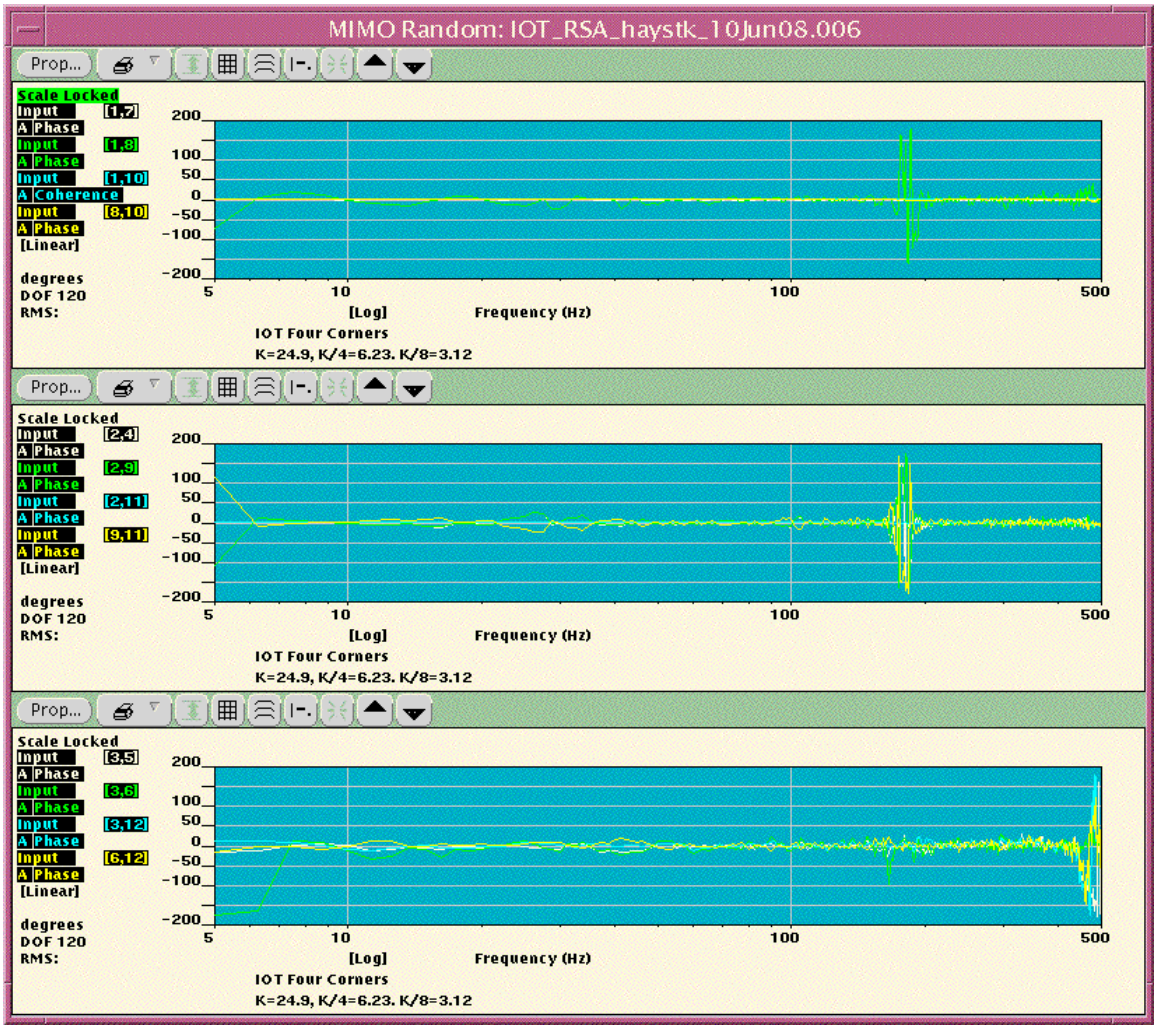

Fig. 21: Selected Phase Responses Between Control Inputs for Test 8

9) I/O Transformation control with pure X, Y, and Z, which are uncorrelated, using 810G spectra, and with controls: x_1, y_1, z_1, y_2, z_2, z_3, x_2, x_3, y_3, x_4, y_4, z_4.

The test configuration for this test is like what we used for test 7) with rectangular control, but with the use of an input transformation, as we used for test 8).

The following Fig. 22 shows the PSD responses we obtained for X, Y, Z, and roll, pitch and yaw. The first three plots show the response for the X, Y, and Z axis that we obtained. The last plot (in the lower right corner) shows the responses for roll, pitch and yaw, which are chosen to be just above the instrumentation's noise floor, which is near 10 rad/sec^2.

Note that with the exception of the power line harmonics at 120 Hz and 180 Hz, and the problem frequency around 185 Hz, the control performance in all 6-DOFs is quite good on the basis of its PSD performance. Also note that the rotational spectra did not use the same references, and thus are not all the same, which is why they appear to be different

above 300 Hz. The rotational references were shaped so that they would be above the instrumentation noise floor, which is the ultimate limit on how well we can suppress rotations. In any case, the rotational responses are within their respective test tolerances.

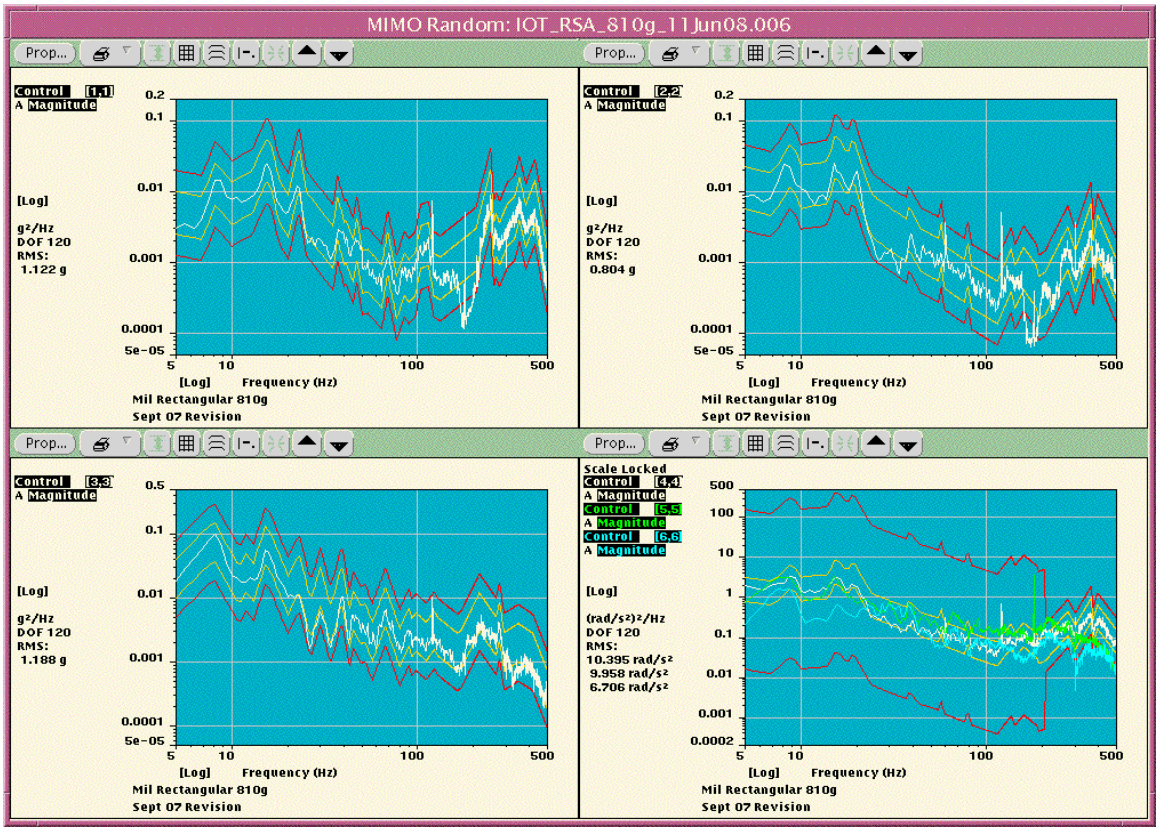

Fig. 22: PSD Responses for the Control DOFs for Test 9

The following Fig. 23 shows the response of the control input accelerometers, before the input transformation. As in Fig. 19, the top plot of Fig. 23 shows the X-axis input channel responses, the middle plot show the Y-axis input channel responses, and the bottom plot shows the Z-axis input channel responses. Again, like axis responses are quite similar to each other, more so than in the rectangular control case, but with a worse performance around 185 Hz. This is probably due to the higher forces needed to restrain unwanted rotations, as compared to rectangular control.

Fig. 23: PSD Responses for the Control Inputs for Test 9

The following Fig. 24 shows the relative coherence between selected control inputs. The top plot shows the relative coherence between selected X-axis responses, the middle plot shows the coherence between selected Y-axis responses, and the bottom plot shows the coherence between selected Z-axis responses. Note that these coherences are better behaved than what we achieved with rectangular control. However, they are worse than what we achieved with the max performance hay-stack spectra references used for test 8). This is probably due to the fact that we're closer to instrumentation's noise floor due to the lower required response at the higher frequencies in the 810G spectra relative to the hay-stack spectra that were used for test 8).

Potential users should note that the instrumentation noise floor requirements for I/O transformation control are more stringent than they are for square and rectangular control. This occurs because we're taking the difference of linear accelerations in order to determine rotational acceleration, as can be seen in the bottom 3 rows of the input transformation matrix shown in (Eq. 1). Noise in this calculation can affect the result much more than the summing operation used to determine the rectilinear accelerations

used to determine: X, Y, and Z, as shown in the top three rows of the input transformation matrix used in (Eq. 1).

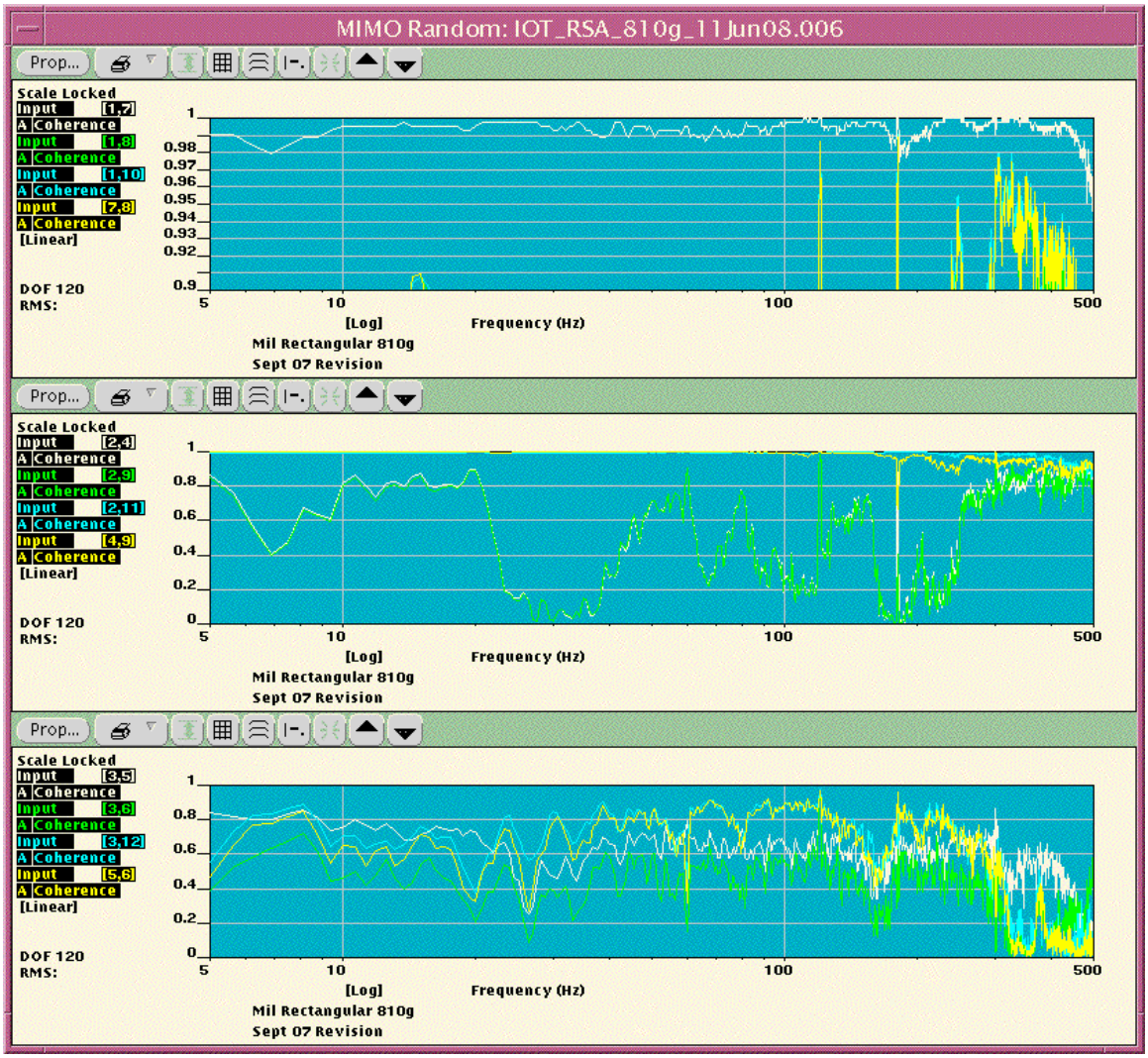

Fig. 24: Selected Coherence Responses Between Control Inputs for Test 9

The following Fig. 25 shows selected relative phase responses between control inputs. The top plot shows the relative phase between selected X-axis responses, the middle plot shows the relative phase between selected Y-axis responses, and the bottom plot shows the relative phase between selected Z-axis responses. Note that these relative phase responses for test 9) are better behaved than what we achieved with rectangular control. However, they are also worse than what we obtained with the haystack spectrum used for test 8), which is probably due to the responses being lower and closer to the instrumentation's noise floor.

In any case, the overall test performance does seem better than what we obtained with rectangular control except for the area around 185 Hz, which is probably due to the fact that we were pushing the Cube much harder with this test, because the I/O transformation control methodology actively suppresses rotations, in this instance, while rectangular

control does this indirectly. This difference thereby requires more force from the Cube, which thus excites the pedestal resonance to a greater degree.

It is felt that this test may require the use of 3-sigma clipping in order to be able to push the Cube harder in order to reach the 810G test's full level. Also, the conservative scaling used in MIMO drive signal synthesis may be a further limit on how high of a level we can achieve on the Cube. Future studies may shed further light on this issue.

Fig. 25: Selected Phase Responses Between Control Inputs for Test 9

Conclusions

The SD JAGUAR controller, using all of the test methods that were discussed, can control the TEAM Cube's responses in 6-DOFs. Also the relative coherence and phase between control responses can also be so controlled up to 500 Hz. This control can be accomplished with under defined and optimal square control; rectangular control; and with I/O transformational control.

Use of under defined square control is not recommended for 6-DOF testing in most cases. Optimal square control is recommended, if control accelerometers are limited and rectangular or I/O transformation tests can't be performed.

Rectangular control works quite well on the Team Cube resulting in the matching of 12 references with only 6 drives. Test results indicate that the top surface of the Cube can move as a rigid body in nearly pure rectilinear motion as a result, where the control provides indirect suppression of rotations. Rectangular Control provides a good method to use for simultaneous MIL-STD-810G random testing of the X, Y, and Z axes.

I/O Transformation Control also works quite well on the Cube, which explicitly enables its 6-DOF capability. This method provides either active suppression or can cause rotations and thus provides a better method for simultaneous MIL-STD-810G random testing of all applicable test axes. It provides results in terms of the familiar rigid-body 6-DOFs. However, care is required in choosing the right type of instrumentation so that its noise floor is below the test's requirements. This consideration of the instrumentation and actuation noise floor is very important for a successful test.

The 810G tests needed more power than what was available from the Team Cube that we used, which required compromises in level and at the lowest frequency. Without increasing the amount of hydraulic power, we may need to enable 3-sigma clipping in the MIMO controller in order to make it easier to reach full-level, but more study is needed in this area before we can be conclusive. Additionally, MIMO Random signal synthesis has to use more conservative signal handling to preclude clipping in its signal synthesis operations, which also limits the maximum test level that is possible for a given amplifier configuration. However, the study has shown that MIMO 810G testing is possible and that it yields more uniform test results than single shaker testing can provide.

The study has also shown that over-determined testing provides the best results. Thus if at all possible, users should use either rectangular control or I/O transformation control to perform these types of tests with the Cube. Thus, we recommend these testing methodologies, whenever it is practical to use them.

References

1. Underwood, Marcos A.; ***Multi-exciter Testing Applications: Theory and Practice***; Proceedings - Institute of Environmental Sciences and Technology; April 2002

2. DOD; **MIL-STD-810G - Test Method Standard for Environmental Engineering Considerations and Laboratory Tests**; http://www.dtc.army.mil/publications/MIL-STD-810G.pdf; 31 Oct 08

3. Hale, Michael and Fitz-Coy, Norman; ***On the Use of Linear Accelerometers in Six-DOF Laboratory Motion Replication: A Unified Time-Domain Analysis***; Proceeding of the 76th Shock & Vibration Symposium; Nov 2005; Phoenix, AZ.

4. Underwood, Marcos A. and Keller, Tony; ***Rectangular Control of Multi-Shaker Systems: Theory and some practical results*;** Journal and Proceedings - Institute of Environmental Sciences and Technology; 2003

5. Underwood, Marcos A. and Keller, Tony; ***Applying Coordinate Transformations to Multi Degree of Freedom Shaker Control***; Proceedings of the 74th Shock & Vibration Symposium; October 2003; San Diego, California.

6. Underwood, Marcos A. and Keller, Tony; ***Understanding and using the Spectral Density Matrix*;** Proceedings of the 76th Shock & Vibration Symposium; October 2005; Phoenix, AZ.

7. Underwood, Marcos A. and Keller, Tony; ***Using the Spectral Density Matrix to Determine Ordinary, Partial, and Multiple Coherence*;** Proceedings of the 77th Shock & Vibration Symposium; October 2006; Monterrey, CA.

8. Harris, C.M., and Piersol, A.G.**; Shock and Vibration Handbook. 5th ed**.; 2001; New York; McGraw-Hill.

9. Ayres, Russell; ***Creating Coordinate Transformation Matrices***; Proceedings of the 78th Shock & Vibration Symposium, November 2007, Philadelphia, PA

10. Fitz-Coy, Norman; Nagabhushan, Vivek; and Hale, Michael T., ***Benefits and Challenges of Over-Actuated Excitation Systems***; Proceedings of the 79th Shock & Vibration Symposium; October 2008, Orlando, FL.